2016

Interleukin-15 Overexpression Attenuates Muscle Fatigue Associated with Murine EO771 Mammary Tumors

Joseph F. Bohlen

Interleukin-15 Overexpression Attenuates Muscle Fatigue Associated with Murine EO771 Mammary Tumors

Joseph F Bohlen

Thesis Submitted
to the School of Medicine
at West Virginia University

in partial fulfillment of the requirements for the degree of

Master of Science in
Exercise Physiology

Emidio E. Pistilli, Ph.D., Chair
Stephen E. Alway, Ph.D.
I. Mark Olfert, Ph.D
Linda Vona-Davis, Ph.D

Department of Exercise Physiology

Morgantown, West Virginia
2016

Keywords: Interleukin-15, Cancer Cachexia, Skeletal Muscle,
Muscle Fatigue, Mitochondria

ABSTRACT

Interleukin-15 Overexpression Attenuates Muscle Fatigue Associated with Murine EO771 Mammary Tumors

Joseph F. Bohlen

Severe muscle wasting and muscle dysfunction (cachexia) are considered incurable complications associated with a wide variety of chronic diseases. This loss of function and severe wasting causes an increase in fatigue in cancer patients, leading to reduced motivation for daily activities, further reducing prognosis for recovery in these patients leading to a severe increase in morbidity. Recent work from our lab suggests Interleukin-15 (IL-15) induces a pro-oxidative state in the muscle, reducing fatigue and promoting a more oxidative phenotype. One proposed mechanism behind this is the observation that IL-15 promotes mitochondrial biogenesis, lending more mitochondria for oxidative metabolic processes. Therefore, we tested the hypothesis that orthotopic implantation of E0771 mammary tumor cells would induce greater muscle fatigue in tumor bearing mice and that muscle-specific IL-15 overexpression would attenuate this cancer-induced increase in muscle fatigability. In our initial study performed in C57BL/6 wild type mice, 4 weeks of E0771 mammary tumor growth induced a significant increase in muscle fatigue along with a significant reduction in mtDNA content, while 2 weeks of growth had no effects on muscle function. This was associated with lesser mRNA expression for IL-15 and IL-15Rα in the muscles of tumor bearing mice. Subsequently, we induced E0771 mammary tumors in muscle-specific IL15 over-expressing mice and littermate control mice for 4 weeks. While muscle fatigue was significantly greater in tumor-bearing littermate control mice compared to littermate control mice without tumors, muscle fatigue was attenuated in muscles from tumor-bearing IL15 over-expressing mice compared to IL15TG mice without tumors. These data highlight IL-15 a potential therapy for reducing fatigue in the weakened/cachectic state. Along with this, IL-15 has been well published with promoting Natural Killer (NK) cell cytotoxicity, increasing immunosurveillance and promoting overall T cell development. This, combine with the pro-oxidative environment make IL-15 an ideal therapy for cancer cachexia. Future studies can look at potential dosing requirements of IL-15 before moving on to clinical trials.

Interleukin-15 Overexpression Attenuates Muscle Fatigue Associated with Murine EO771 Mammary Tumors

Joseph F. Bohlen

Division of Exercise Physiology, West Virginia University School of Medicine

Interleukin-15 Overexpression Attenuates Muscle Fatigue Associated with Murine EO771 Mammary Tumors

Joseph F. Bohlen

Division of Exercise Physiology, West Virginia University School of Medicine

Chapter 1.

Introduction:

Severe muscle wasting and muscle dysfunction (cachexia) are considered incurable complications associated with a wide variety of chronic diseases. Cachexia significantly decreases the quality of life for cancer patients, more specifically; it leads to an overall poor prognosis for recovery and accounts for ~40-50% of cancer patient morbidity. (1) Cachexia is classified by a severe loss of body weight due to a significant loss of fat and muscle mass. More pertinent to this study, however, is the muscular dysfunction (fatigue) that is associated with this disease. Cachexia is considered a factor in determining cancer-related death, yet no direct experimental evidence has surfaced to solidify this hypothesis. (2) It has been well documented that standard nutritional approaches do not mediate muscle wasting in regards to cancer. (3,4) In lieu of this, significant focus has shifted towards other strategies for reducing cachexia in cancer patients in order to improve prognosis.

Cancer cachexia is believed to induce muscle wasting, along with muscle dysfunction eliciting significant fatigue and reduced motivation for daily activities. This

fatigue is thought to be derived from alterations in skeletal muscle contractile machinery along with alterations in mitochondrial function. Indeed, cachectic muscles show a shift in fatigue resistance, exhibiting a more glycolytic and fatigable phenotype in muscle fibers. Recent data from our lab suggest IL15 might be an excellent therapy, with potential to reduce the outcomes of cancer cachexia. For example, recently our pilot studies have shown that IL-15 promotes a more oxidative/fatigue resistant phenotype. In addition, our IL15 transgenic overexpressor mice have shown marked increases in markers of mitochondrial biogenesis along with increases in cage activity due to higher levels of circulating IL15. In relation to muscle mass, IL-15 has been shown to cause skeletal fiber growth and stimulate myogenic differentiation (5,6). IL-15 has also been shown to have a profound effect on the immune system, stimulating NK cell cytotoxicity, increasing immunosurveillance and protecting from tumor development (7). Therefore, our central hypothesis is that overexpression of IL-15 will preserve muscle function, along with increasing the immuneosurveillance of T cells and NK cells, there by attenuating cancer cachexia and the subsequent severe tumor progression. Currently, we have bred an IL15 skeletal muscle overexpressor mouse that we will inject with the EO771 adenocarcinoma cell line in order to examine the effects of IL15 overexpression on cancer cachexia. We used these mice in conjunction with our background in muscle testing to address our hypothesis by completing the following aims.

Aim 1: **Determine the effects of IL15 skeletal muscle overexpression on muscle weight and muscle dysfunction seen in cancer cachexia**.

Our working hypothesis is that IL 15 overexpression will preserve muscle function in the presence of cancer cachexia. From our preliminary data, we know the EO771 breast cancer cell line causes increased muscle dysfunction along with significant muscle wasting. We expect to see a preservation of muscle force and a resistance in fatigue in the presence of IL15 overexpression in tumor bearing mice.

Aim 2: **Determine the effects of IL15 skeletal muscle overexpression on cell populations in the spleen and infiltrating spleen cells in the solid tumor.**

Our working hypothesis is that IL15 overexpression will stimulate an increase percentage of Cytotoxic and Helper T cells and NK cells in both the spleen and tumor of the transgenic mouse. Due to the ability of these cells to combat tumor formation and metastasis, we believe IL15 overexpression will reduce severity of tumor progression and symptoms experienced during cancer cachexia.

Chapter 2.

Background:

2.1

Cancer Cachexia

Cancer is responsible for nearly 1,500 deaths every day, with fifty percent of these patients experiencing cachexia (8). Cachexia is generalized as a weakness and wasting induced by a severe chronic illness. The effects of cachexia are often exacerbated by the disease itself creating a self-sustaining loop. One key component of cancer cachexia is the extreme depletion of skeletal muscle mass compounded with profound fat loss, along with severe fatigue in patients (2). The main contributors to this disease are believed to be abnormal fluctuations in cytokines, hormones and tumor derived factors that alter the cellular environment (9). Cancer cachexia is not limited to skeletal muscle alterations, this disease is also associated with neuroendocrine disorder, systemic inflammation, fat atrophy, and overall metabolic dysfunction (10).

Current treatment for cancer cachexia is multimodal in nature. The basics include nutritional intervention along with supplemented exercise in order to stave off the wasting effects(11,12). While these treatments do little to reverse the effects of cancer cachexia, they can potentially reduce the symptomology in some cases (13). The significant problem with traditional treatment methods for cancer (i.e. chemotherapy, radiotherapy) is the exacerbation of cachexia, further decreasing the prognosis of survival after treatment (14). Recent drug trials in rats revealed a potential combination therapy that could alleviate the cachectic effects of cancer all

while reducing tumor burden (15). The problem with this treatment is that these drugs could have severe adverse effects in human subjects. Thus, it becomes critical to discover treatment options that attenuate these adverse reactions allowing other primary treatment to reduce tumor burden and move the cancer into remission.

2.2

Biomarkers and Indicators of Cancer Cachexia

Markers of inflammation, skeletal muscle degradation markers and tumor derived compounds all show some degree of significance in regards to cancer cachexia and subsequent pathways of fatigue (16). The main biomarkers we are concerned with in this instance are; Atrogin-1, Murf-1, TNFα, IL-6, IL-15 and IL-15rα. TNFα has long been considered one of the more prominent indicators of cancer cachexia. This proinflammatory cytokine is believed to play a role in growth and angiogenesis/metastasis of cancer cells (17). More importantly high levels of TNFα have been linked with remodeling of stromal development along with being an endogenous tumor promoter (18). There is evidence that suggests the pro-inflammatory cytokine IL-6 also plays an important role in cancer cachexia (19). While a main indicator of cachexia, IL-6 is believed to mediate the acute phase response involved with early infection and inflammation (20). With progression of disease however, IL-6 has been shown to increase and inhibit cancer cell apoptosis and create drug resistance (21). Atrogin-1 and Murf-1 have both been identified as muscle-specific E3 ubiquitin ligases that are transcriptionally increased in the presence of

atrophy/atrophy-induced conditions (22). These markers are enriched in skeletal muscle making them excellent markers of muscle atrophy in relation to cancer cachexia. IL-15, as previously mentioned, promotes mitochondrial biogenesis and fatigue resistant properties. Along with this, IL-15 has a highly specific binding partner IL-15rα. When bound together, they have the ability to act directly on skeletal muscle in a pro-oxidative manner (23). Decreases in these two markers could possibly be a mechanistic link between the increases in fatigue found in cancer cachexia with the decrease in mitochondrial biogenesis.

Importantly, cancer cachexia can be identified by decreases in bodyweight associated with severe loss of adipose tissue and muscle mass (9). Measuring bodyweight is an easy and noninvasive way to gauge progression. Measuring cross sectional area of a muscle section however, can provide a more comprehensive measurement of muscle wasting. Indeed, cancer cachexia has been found to decrease cross sectional area with progression of disease, yielding more fibers that are smaller in size (24,25). This can yield a muscle that fails to generate maximal amounts of force like their non-cachectic counterparts.

2.3

Immune Function during Cancer Cachexia

Natural Killer (NK) cells express the ability to target specific cells without the need for antibody recognition (26). In higher concentrations NK cells can identify and kill foreign pathogens increasing the productivity of the immune system (27). Another

key component in immune function is the Helper and Cytotoxic T Cells. Specifically, Helper T cells (CD4+) play a central role in regulating nearly all antigen-specific immune responses to invading pathogens (cancer cells)(28). Just as important are the Cytotoxic T cells (CD8+), being able to induce tumor cell death upon direct recognition of peptide antigens (29). Stemming from the alterations in skeletal muscle comes further dysfunction in the way of the immune response to cancer cachexia. The alterations associated with cancer cachexia mostly affect innate responses to pathogens both in the tumor and systemically (30). A large issue with many cancers is the ability of the cells themselves so shed antigens or even promote T cell and NK cell lysis (31). Another mechanism blunting immune response is the tumors microenvironment preventing expansion/proliferation of helper and cytotoxic T cells, all while increasing the pro-inflammatory response causing eventual suppression of these cell types (32).

The problem with treating cancer with one specific drug is that it can alter a patient's physiological homeostasis. Complications can arise with drugs that target the cancer cells or specific symptoms of cancer cachexia (anorexia) (33). One major adverse effect is immune suppression, which further inhibits the body's response to invading pathogens increasing morbidity (34). The inflammation response to cancer cachexia mainly involves the previously mentioned pro-inflammatory cytokines IL-6 and TNFα. TNFα has been shown to promote adhesion of free floating tumor cells along with promoting malignancy (35,36). IL-6 shows similarities, promoting both cancer cell growth, along with resistance to therapy (37). With these alterations to immune function, along with the increase in fatigue from cancer cachexia, an ideal treatment is needed that can alleviate these symptoms without exacerbating the cancer itself.

2.4

IL-15s Role in Cancer Cachexia

The primary goal of this research is to ascertain the ability of IL-15 to attenuate muscle fatigue and maintain immune function during progression of cancer. If confirmed IL-15 therapy would complement other treatments in the reduction of cancer, increasing longevity and survival rates among patients. IL-15 is a recently discovered four-helix bundle cytokine (38). Skeletal muscle is considered to have the largest pool of IL-15 mRNA, with increases in systemic IL-15 exhibiting a pro-oxidative environment (39,40). Therefore, we proposed the use of an IL-15 overexpressor mouse in order to test the effects of IL-15 during a cachectic state. IL-15 has been shown to promote a pro-oxidative phenotype in skeletal muscle creating fatigue resistance along with increasing markers for mitochondrial biogenesis (41). With the increased mitochondria biogenesis, muscle fatigue would be reduced. This proposed shift in mitochondria volume could potentially alleviate any fatigue induced by cancer cachexia.

Il-15 is believed to promote maturation in NK cells and T cells, allowing for an increased immune response in association with invading pathogens (42). Along with this, IL-15 would promote greater immunesurveillance and encourage infiltration of the primary tumor, reducing overall tumor burden (42-44). Understanding how IL-15 overexpression effects cancer cachexia in a mouse model is the first step in identifying its effectiveness as a supplemental therapy. We expect that our research will identify IL-15 as a mitigator of cancer cachexia, reducing overall severity and associated

symptomology. Upon the conclusion of the proposed study, we will have a feasible idea of the next steps needed in order to apply this to a clinical environment.

2.5

Background summary, aims, and hypothesis

The symptomology of cancer cachexia brings about multiple complications that can lead to early morbidity. The primary goal of this research is to solidify a treatment method which attenuates cachexia. Once established, we will than look into clinical dosing aspects and potential combination therapy to than reduce tumor burden and more importantly reduce the rate of muscle fatigue. We expect that our research will identify IL-15 as a mitigator of cancer cachexia, reducing rate of muscle fatigue and increasing the immune response to the tumor. With increasing circulating levels of IL-15 comes an increase in biomarkers of mitochondrial biogenesis (i.e. PGC-1α, PPARα/δ). Through transcriptional activation and increased signaling comes a subsequent increase in the amount of mitochondria per cross sectional-area. This creates a more oxidative fiber type in skeletal muscle, promoting a fatigue resistant phenotype. IL-15 is already well-published in promoting immunosurveillance through proliferative effects on NK cells and cytotoxic CD8 T cells.

With this in mind this project has two specific aims: first, determine the effects of IL-15 overexpression on reducing the rate of muscle fatigue, and second, to determine the effects of IL-15 overexpression on NK cell and T cell populations in the spleen and tumor of injected mice. For these two aims, we injected IL-15 skeletal muscle

overepressor mice and litter controls with the EO771 adenocarcinoma cell line. The EO771 cell line is ER-positive and immunosuppressive in nature. After 4 weeks all tissues and muscle were collected and analyzed. It was hypothesized that IL-15 skeletal muscle overexpression would attenuate the increased rate of muscle fatigue experienced in cachectic tumor burdened mice when compared to littermate controls. Furthermore, it was hypothesized that IL-15 skeletal muscle overexpression would increase NK cell and T cell count in the spleen and tumor when compared to littermate controls.

Chapter 3

The EO771 Adenocarcinoma Breast Cancer Cell Induces Cancer Cachexia at 4 Weeks in C57BL/6WT Mice.

Joseph F. Bohlen[1], Sarah A. McLaughlin[3], Sijin Wen[4], Emidio E. Pistilli[1,2]

1 West Virginia University School of Medicine, Division of Exercise Physiology; 2 Center for Cardiovascular and Respiratory Sciences; 3 Mary Babb Randolph Cancer Center; 4 Department of Biostatistics

The EO771 Adenocarcinoma Breast Cancer Cell Induces Cancer Cachexia at 4 Weeks in C57BL/6WT Mice.

Severe muscle wasting and muscle dysfunction (cachexia) are considered incurable complications associated with a wide variety of chronic diseases. Cachexia significantly decreases the quality of life for cancer patients; more specifically, it leads to an overall poor prognosis for recovery and accounts for ~40-50% of cancer patient morbidity. Cachexia is classified by a severe loss of body weight due to a complete loss of fat and, more pertinent to this study, profound loss of skeletal muscle mass. Breast cancer is considered the most frequently diagnosed cancer in females accounting for 14% of cancer deaths with ~27% of these patients experiencing cachexia. Therefore, we hypothesize that mice with severe cancer cachexia following 4 week cell injection (EO771) will show decreases in force production along with decreased fatigue resistance. **PURPOSE:** To determine whether the EO771 cell line induces a solid tumor and subsequently causes cancer cachexia altering muscle weight and function. **METHODS:** C57BL/6WT female mice were split into three groups consisting of an un-injected control group (n=8), a 2 week post injection group (n=5) and a 4 week non-ulcerated tumor (n=4) and ulcerated tumor post injection group (n=6). Isometric force and fatigue properties were determined in EDL and soleus muscles ex vivo while all other muscles and organs were dissected and weighted. RNA was isolated from tibialis anterior muscles and reverse transcribed for semi quantitative PCR. DNA was isolated in order to look at mitochondrial DNA content using RT-PCR. **RESULTS:** 4WK ulcerated EDL muscles showed a significant decrease in tetanus force (CON 214.0 ±

23.26 nM vs. 4WK ulcerated 149.9 ± 42.58 nM, $p<0.0001$) with a shift in the force frequency curve, along with significant loss of muscle mass compared to both the CON and 2WK time point(CON 10.58 ± 1.152 mg vs. 4WK ulcerated 7.325 ± 0.9621mg, $p<0.0001$). 4WK mice also showed increases in markers for inflammation and muscle atrophy **CONCLUSION:** The results of this study suggest that the EO771 cell line does in fact induce cachexia. The decrease in muscle weight, along with an increase in fatigue coincides with the symptomology of cancer cachexia. Furthermore, the increases in inflammatory markers, atrophy markers highlight the physiological alterations taking place in this disease. Methods of therapy can now be applied to this particular cell line when considering attenuation of cancer cachexia.

INTRODUCTION

Severe muscle wasting (cachexia) is considered an incurable complication associated with a wide variety of chronic diseases. Cachexia significantly decreases the quality of life for cancer patients; more specifically, it leads to an overall poor prognosis for recovery and accounts for ~40-50% of cancer patient morbidity(1). Cachexia is classified by a severe loss of body weight due to a complete loss of fat and, more pertinent to this study, profound loss of skeletal muscle mass. The symptomology of this disease includes fatigue, anorexia and abnormal biochemistry, in turn altering several metabolic pathways in tissues and organs. (2,3) Generalized circulating factors such as tumor derived compounds, inflammatory cytokines, acute phase proteins and skeletal muscle degradation markers all play significant roles respectively. (3) Specifically, TNF α and IL – 6 have been documented to increase progressively along with the severity of cancer (4). Markers of acute muscle atrophy such as, MAFbx/Atrogin-1 and Murf1 have also shown upregulation in multiple models of cancer (5). The downstream effect of these factors is usually a loss of myofibrillar proteins in muscle cells resulting in muscle weakness and fatigue. This is exacerbated by the increase in apoptosis compounded with impaired regeneration capabilities seen in cancer patients(6). Interestingly cachexia has shown selective atrophy in fast glycolytic fibers, associated with increases in proinflammatory cytokines (7).

One possible mechanism behind the cachectic fatigue resides in alterations in mitochondrial function. Considered multi-functional organelles, mitochondria provide a majority of the ATP in cells along with participating in a plethora of signaling cascades, including apoptosis. In a Lewis Lung Carcinoma model, mitochondrial ATP synthesis was shown to decrease suggesting mitochondrial dysfunction as the potential cause for muscular fatigue (8). Circulating factors produced by cancer cells have also shown to alter electron transport chain (ETC) activity, reduce basal respiration, along with potentially creating a self-amplifying loop of oxidative stress (9).One implication behind this is the upregulation of reactive oxygen species (ROS), signaling the induction of tumorigenesis and metastasis (10). UCP3, the predominant uncoupling protein in skeletal muscle, has also shown marked alterations. Increases in amount and activity of UCP3 show reductions in proton gradient across the inner mitochondrial membrane. This increases energy expenditure via the dissipation of energy as heat (11).

Breast cancer is considered the most frequently diagnosed cancer in females accounting for 14% of cancer deaths (12). Traditional interventions do little to attenuate the progressive wasting associated with cancer cachexia. There is a general decrease in food intake, compounded with a state of hypermetabolsim that yields standard nutritional approaches futile (13). Therefore, it becomes pertinent to identify ideal mouse models of cachexia in order to test feasible methods of treatment that do not exacerbate these wasting symptoms. In this study we examined the effect of the EO771 breast cancer cell line on initiation of muscle wasting and dysfunction in C57BL/6 WT mice. The EO771 breast cancer cell line is aggressive and proliferates rapidly. In this case we wanted to show solid tumor development in immunocompetent

mice looking at metastases, muscle wasting/dysfunction, tumor burden and metabolic alterations following 2 and 4-week tumor bearing periods. We hypothesize that mice with severe cancer cachexia will show decreases in force production along with decreased fatigue resistance. Concluding this study, we plan to identify this as an ideal model for use when studying breast cancer cachexia looking for potential therapies to attenuate the downstream alterations.

METHODS

Mice

C57BL6WT mice were purchased from The Jackson Laboratory (n=23) and randomly assigned to a control group (Control; n=8), mice that were euthanized following 2 weeks of tumor growth (2WK, n=5), and mice that were euthanized following 4 weeks of tumor growth (4WK, n=10). The 4WK group was subsequently divided into mice that developed an ulcerated tumor (4WK-UT; n=6) and mice that developed a non-ulcerated tumor (4WK-NUT; n=4). Mice were housed in the animal vivarium at West Virginia University at 22°C under a 12:12-h light-dark cycle and received food and water ab libitum. All animal experiments were approved by the Institutional Animal Care and Use Committee at West Virginia University.

E0771 Murine Breast Cancer Cells

The E0771 cell line used in these studies was kindly provided by Dr. Metheny-Barlow from Wake Forest University. E0771 cells were cultured using aseptic technique and maintained under standard mammalian culture conditions (37ºC, 99% humidity, 5% CO_2). Cells were maintained in high glucose DMEM supplemented with 10% FBS to maintain active proliferation. Cells were passed via trypsinization using 0.25% trypsin/EDTA in Hanks buffered saline solution (Gibco). Cells were grown until ~90% confluent at which time they were prepped for injection. Cells were trypsinized and resuspended in sterile PBS. A cell count was performed yielding 1 million cells per 100µL injection into the 4^{th} nipple (mammary fat pad) of female C57BL/6 WT mice.

In vivo tumor bioluminescence and volume measurements.

Mice were injected with luciferase-expressing EO771 breast cancer cells and imaged weekly for quantitative evaluation of tumor growth and dissemination. About 150 mg/kg D-luciferin (Caliper Life Sciences) was injected into the peritoneum. Images were obtained using the IVIS Lumina-II Imaging System and Living Image-4.0 software (14).

Ex vivo muscle physiological analysis

Muscle contractile properties were examined in the fast extensor digitorum longus (EDL) and slow soleus muscles of experimental mice. Mice were deeply anesthetized by breathing 4% isoflurane delivered through a nose cone at a flow rate of 1 l/min. Muscles were removed with both proximal and distal tendons intact, and nylon sutures were attached to the tendons. Muscles were transferred to an oxygenated tissue bath that contained Ringer solution (100 mM NaCl, 4.7 mM KCl, 3.4 mM CaCl2, 1.2 mM KH2PO4, 1.2 mM MgSO4, 25 mM HEPES, and 5.5 mM D-glucose) maintained at 22°C. Ex vivo muscle stimulation was performed using a commercially available muscle physiology system (Aurora Scientific, Ontario, CA). Muscle length was adjusted to obtain the maximal twitch response (i.e., Lo). Three twitch contractions were performed all separated by 2 min. Parameters analyzed from isometric contractions included peak isometric twitch force (Pt), time to peak twitch tension (TPT), half-relaxation time of twitch contraction (½ RT), and peak isometric tetanic force (Po). Isometric tetanic contractions were stimulated in muscles at a stimulation frequency of 120 Hz for EDL muscles and 80 Hz for soleus muscles, a stimulation current of 20 V, and lasting 500 ms. Following isometric contractions, the muscles remained in oxygenated Ringer's for

5 minutes prior to the repeated-stimulation fatigue protocol. Muscle fatigue was analyzed using a repeated stimulation protocol lasting 6 min and consisting of repeated 40-Hz tetanic trains that occurred once every second and lasted 330 ms. The fatigue index was calculated as the difference in force from the first contraction and every tenth subsequent contraction, and plotted as a fatigue curve. (Burke1973, Pistilli 2011) Muscles were flash frozen in isopentane cooled to the temperature of liquid nitrogen and stored at –80°C. Muscle CSA was calculated by dividing the muscle mass by the product of the muscle density coefficient (1.06 g • cm3), muscle Lo, and the fiber length coefficient (EDL: 0.45, soleus: 0.69). This whole muscle CSA value was used to calculate specific force (i.e., absolute force mN • muscle CSA–1) (Brooks 1988, Lynch 2001)

Muscle Histology and Morphology

Serial frozen sections (10 μm thick) of EDL and SOL muscles were obtained using a cryostat at −21°C and placed onto glass slides (Superfrost/Plus, Fisher Scientific). Sections were stained with Alexa Flour® 488-conjugate AffiniPure Goat Anti-Rabbit IgG (Jackson ImmunoResearch Labratories, INC) and ANTI-LAMININ Affinity Isolated Antigen Specific Antibody(SIGMA-ALDRICH®) and then mounted with 4’,6-diamidino-2-phenylindole (DAPI) mounting medium (Vector Laboratories, Burlingham, CA).

Mitochondrial DNA content

Total DNA (genomic and mitochondrial) was extracted from tibialis anterior (TA) muscles from female mice using a DNeasy Blood and Tissue kit (Qiagen, Valencia, CA)

and quantified using a Nano-Drop spectrophotometer (ThermoScientific, Waltham, MA). TaqMan primers for mitochondrial DNA-encoded cytochrome-c oxidase subunit II (COXII) and nuclear-encoded 18S ribosomal RNA were used to perform real-time qPCR. The wells of a 96-well optical reaction plate were loaded with a 20-µl volume consisting of TaqMan 10X PCR Master Mix, a primer mix for either the mitochondrial-encoded gene or the nuclear-encoded gene, and DNA diluted to a concentration of 5 ng/µl. Each DNA sample was analyzed in pairs and amplified in an Applied Biosystems 7900HT Fast Real-Time PCR system. The cycle threshold (CT) values of the mitochondrial-encoded COXII gene and the nuclear-encoded 18S gene in muscles C57BL/6 WT mice were used to quantify the fold change using the ΔΔCT calculation (Livak 2001).

mRNA Analysis

Total RNA was isolated using Trizol reagent (Life Technologies, Grand Island, NY), as previously described (15). RNA quantity and quality were assessed using a Nano-Drop 2000 spectrophotometer (ThermoScientific, Waltham, MA); the 260/280 ratio for all samples used was between 1.8 and 2.1. Two micrograms of total RNA was reverse transcribed to make cDNA using a high-capacity reverse transcription kit according to manufacturer's instructions (Life Technologies, Grand Island, NY). Amplification was performed in a reaction consisting of 8.5 µl nuclease-free H2O, 12.5 µl 2X Taq-Pro Red Complete 1.5 mM MgCl2 master mix (Denville Scientific, Metuchen, NJ), 1.0 µl forward primer, 1.0 µl reverse primer, and 2 µl of DNA template to make a 25 µl total reaction volume. Primers were constructed from published sequences. Primer pairs for IL-15,

IL-15 rα, IL-6, TNFα, Murf1 and Atrogin-1 were coamplified with primer pairs for 18S (Ambion, Austin, TX). The number of PCR cycles was determined in preliminary experiments to ensure analyses were done in the linear range of amplification. Following amplification, each reaction was visualized following gel electrophoresis in 1% (wt/vol) agarose gels stained with ethidium bromide. PCR bands were quantified using the ImageJ software program (http://rsbweb.nih.gov/ij/). Signals for the gene of interest were normalized to the bands for 18S that were amplified in the same reaction.

Spleen Cell Isolation

Spleens were dissected from mice and spleen cell populations were isolated by creating a cell suspension in 1.5% FBS RPMI. Cells were then passed through a 70µm filter into a new tube. Red blood cells were lysed by adding 4 mL of fresh Tris-NH_4Cl at room temperature and letting stand for 3 minutes. Tris- NH_4Cl was inhibited with 5 mL of 10% FBS RPMI and two washing steps performed using 1.5% FBS RPMI. A cell count was performed yielding 1 million cells per vial. Samples were than stored in 0.5% paraformaldehyde until being re-suspended in FACS buffer for flow cytometry analysis.

RESULTS

In vivo tumor burden. One million E0771 tumor cells were implanted into the mammary fat pads of female wild type C57BL/6 mice and cell bioluminescence and tumor volume were monitored weekly. As seen in **Figure 1A**, representative images display a progressive increase in cell bioluminescence and tumor size through four weeks.

E0771 tumor induced alterations in body and muscle mass. The body mass of female C57BL6 following 2 weeks of tumor growth was not significantly different from control non-tumor bearing mice. However, the body mass of mice following 4 weeks of tumor growth was 28% less than both control and 2 week mice. The masses of individual skeletal muscles of the lower limb all displayed a similar response pattern. The normalized muscle masses of muscles from female C57BL6 mice following 2 weeks of tumor growth was not significantly different from control non-tumor bearing mice **(Figure 8).** The normalized muscle masses in mice following 4 weeks of tumor growth were significantly less than control mice and mice following 2 weeks of tumor growth **(Figure 8)**. The absolute and normalized mass of the spleen was greater in mice following 4 weeks of tumor growth compared to control mice and mice following 2 weeks of tumor growth. **(Figure 8E)**

Fatigue properties. Muscle fatigue was analyzed using a repeated stimulation protocol, with the fatigue index calculated as the percent difference of each contraction from the initial contraction of the protocol. When the fatigue index was plotted, a clear

pattern emerged with respect to the duration of tumor exposure. The fatigue index curve of EDL muscles from mice exposed to 4 weeks of tumor growth was shifted to the left during the initial 20-70s of the protocol compared to the fatigue index of EDL muscles from control mice and mice exposed to 2 weeks of tumor growth, indicating a significant loss of force with repeated contractions during this timeframe. There were no differences in the fatigue index curve of EDL muscles from control mice compared to mice exposed to 2 weeks of tumor growth **(Figure 4A)**. The total area under the curve (AUC) was calculated for each fatigue curve. Supporting the fatigue curves, there was a significantly lower AUC when comparing the fatigue curves of EDL muscles from mice exposed to 4 weeks of tumor growth to control mice. In the soleus muscle, there were no significant differences between the groups in the fatigue index **(Figure 4B)** or the AUC. The mtDNA content, as assessed by qPCR, showed a statistical significance for a reduction in muscles from mice exposed to 4 weeks of tumor growth compared to muscles from control mice, suggesting the duration of tumor growth affected mitochondrial density in skeletal muscles **(Figure 4C)**.

Isometric force production. The CT of EDL muscles was significantly longer in mice following 4 weeks of tumor growth compared to control mice **(Figure 2C)**. The 1/2RT of EDL muscles was also longer in mice following 4 weeks of tumor growth compared to control mice **(Figure 2D)**. Absolute maximal tetanus force of EDL muscles was significantly lower in mice following 4 weeks of tumor growth in the ulcerated group compared to control, 2WK and 4WK non-ulcerated mice **(Figure 3C)**. Absolute tetanus force was also significantly lesser in EDL muscles from 4 week ulcerated tumor mice at

stimulation frequencies of 80, 100, 120, and 150Hz **(Figure 3A)**. When the force-frequency relationship was expressed as force normalized to maximal force, there was a significant leftward shift of the relationship, such that force was significantly different in 4 week mice at stimulation frequencies of 1, 5, 10, and 25Hz **(Figure 3B)**.

There were no differences in the CT or 1/2RT of twitch contractions in SOL muscles **(Figures 2G, H**). Absolute maximal tetanus force was significantly lower in 4WK mice compared to control and 2 week mice **(Figure 3F)**. Absolute tetanus force was also significantly lesser in SOL muscles from 4WK mice at stimulation frequencies of 50, 80, and 100Hz **(Figure 3D)**. There were no differences in the force-frequency relationship when expressed as force normalized to maximal force **(Figure 4F)**.

Single Fiber Area Analyzing cross sectional area (CSA) following laminin staining we saw a significant shift in the 2WK and both 4WK groups to the left in the EDL muscles, indicating a greater percentage of smaller fibers in these muscles in response to cancer. **(Figure 6 A, B)** No shift was seen on the SOL muscles for any groups **(Figure 6 C, D)**

mRNA Expression Control mice showed the highest levels of IL-15 and IL15rα. In regards to IL-15 there was a linear decrease in skeletal muscle expression, with the 4 week groups expressing the lowest amount **(Figure 5C)**. IL-15 rα showed a significant decrease in 2week and both 4 week groups when compared to control mice **(Figure 5F)**. IL-6 expression increased linearly with progression of cancer, with the 4 week ulcerated group having significantly high levels (**Figure 5 B)**. While TNF α did show marked increase, levels in the 4 week ulcerated group did not reach significance(**Figure**

5 E). Atrogin 1and Murf 1 showed a significant increase in the 4 week ulcerated group when compared to all other groups (**Figure 5 A, B)**.

IVIS Imaging Tumor progression increased linearly from week to week. These data were confirmed with caliper measurements ($0.5236 \times W^2 \times L$) looking at the volume of the tumor (**Figure 7B)**. The photon flux from the tumor is proportional to the number of light emitting cells and the signal can be measured to monitor tumor growth and development (Lim 2009) **(Figure 7C)**. Flux numbers began an exponential increase at the 3 and 4WK time points verifying the increase in tumor growth. At the 4WK time point there was a contrast between large solid tumors and smaller necrotic tumors containing ulcerations **(Figure 7 A, B)**. These data indicate a differentiation in response to the Eo771 cell line.

Spleen Cell Percent No significant differences were seen between T cell or NK cell populations **(Figure 9 A, B).** A t-test between the CON and 2WK groups revealed a significant decrease in T cell % at the 2WK time point.

DISCUSSION

The profound muscle wasting from cancer cachexia is associated with muscle weakness and reduced strength (16). Many attribute muscle wasting as the main contributor to the decrease in strength and muscle weakness, some studies suggest additional factors that contribute to the alterations in excitation-contraction coupling and development of force (17). Inflammatory cytokines secreted by and in response to tumors have been shown to directly induce signaling pathways that have been shown to upregulate enzymes that induce skeletal muscle protein turnover (18). Specifically, in this model there is a significant increase in IL-6 in the 4WK Ulcerated group, one of the main inflammatory markers in cancer cachexia. While there was no significant difference in TNF α in skeletal muscle, there was a greater increase in the 4WK Ulcerated group. These data indicate the 4WK Ulcerated group having a more severe response to the cancer and a subsequent increase in cachexia. Significant increases in Atrogin1 and Murf1 along with decreases in fiber area and single fiber CSA in all cancer groups in the EDL muscle coincide with muscle atrophy seen in cancer cachexia. While not entirely similar to muscular dystrophy loss of dystrophin protein is associated with increases in MuRF1/Atrogin1activity increasing myofibrillar protein breakdown (19). Furthermore, muscle weights for the Gastrocnemius, Tibialus Anterior, Quadriceps, Plantaris, EDL and SOL showed significant decrease in the 4-week time point, even when normalized to overall body mass, indicating this cancer cell line having a cachectic effect on muscle mass. Indeed, mice in the 4WK Ulcerated group experienced severe cachexia illustrated by weight loss measured after tumor removal. EDL muscles showed increased CT and 1/2RT indicating alterations in calcium handling

with the contractile machinery, further contributing to muscle dysfunction. EDL force frequency expressed as force normalized to maximal forces expressed a significant leftward shift in both 4WK groups indicating these muscles are producing lower force. Furthermore, the EDL of 4WK mice had a significant drop in force from 30-70 contractions during the fatigue protocol indicating a significant increase in fatigue in these mice. This shift further exemplifies the contractility alterations seen in many cancer cell lines that exhibit a cachectic/dysfunctional effect (17). Il- 15rα has been implicated as being a binding partner for IL-15, increasing biological activity and half-life of IL-15 (20). In our model we show significant decreases in IL-15 and IL-15rα mRNA levels in all cancer groups. Furthermore, decreases in IL-15 and IL-15rα can be associated with a decreased rate of mitochondrial biogenesis contributing to the increase in fatigue seen in the EDL muscles at 4WK time point. This decrease yields potentially less functional mitochondria decreasing the overall oxidative capacity of the muscle (8, 9, 10). Indeed, the mtDNA assay showed significant decreases in genomic DNA in both 4WK time points coinciding with our fatigue data. While SOL muscles did experience a decrease in max tetanic force at both 4WK time points and a significant decrease in weight at the 4WK Ulcerated time point, all other physiological parameters were unchanged. This is supported by previous work showing preservation in a more oxidative muscle in cancer cachexia (7). Spleen cell data showed do differences between groups in T cell% or NK cell%. This perhaps could be due to a small sample size or the immunosuppressive nature of this cell line at later stages of development (21).

These data highlight a clear separation in progression and severity of cancer cachexia. There was a clear delineation at the 4WK time point leading to two different phenotypic responses to the E0771 cell line which can be representative of ~40-50% of cancer patients (1). Our 4WK Ulcerated mice showed significant increases in transcriptional markers of inflammation, atrophy along with a significant decrease in tetanic force combined with an increased rate of fatigue associated with a decrease in mtDNA content. While our 4WK Non-Ulcerated group did exhibit similarities in fatigue and mtDNA content, we saw no significant differences in our markers for atrophy and inflammation along with no differences in maximal tetanic force. In conclusion we establish that the EO771 adenocarcinoma cell line produces a solid tumor increasing in size with progression of disease. At the 4WK time point mice exhibited signs and symptoms of cancer cachexia supported by the decrease in force output, increased rate of muscle fatigue and decrease in muscle mass. These data indicate the EO771 cell line is ideal for use in determining the effects of certain therapies on cancer cachexia.

Refrences

1. Tisdale, M. J. (2002) Cachexia in cancer patients. *Nature Reviews Cancer* **2**, 862-871

2. Argiles, J. M., Busquets, S., Stemmler, B., and Lopez-Soriano, F. J. (2014) Cancer cachexia: understanding the molecular basis. *Nature reviews. Cancer* **14**, 754-762

3. Evans, W. J., Morley, J. E., Argiles, J., Bales, C., Baracos, V., Guttridge, D., Jatoi, A., Kalantar-Zadeh, K., Lochs, H., Mantovani, G., Marks, D., Mitch, W. E., Muscaritoli, M., Najand, A., Ponikowski, P., Rossi Fanelli, F., Schambelan, M., Schols, A., Schuster, M., Thomas, D., Wolfe, R., and Anker, S. D. (2008) Cachexia: a new definition. *Clinical nutrition* **27**, 793-799

4. Michalaki, V., Syrigos, K., Charles, P., and Waxman, J. (2004) Serum levels of IL-6 and TNF-alpha correlate with clinicopathological features and patient survival in patients with prostate cancer. *British journal of cancer* **90**, 2312-2316

5. Gomes, M. D., Lecker, S. H., Jagoe, R. T., Navon, A., and Goldberg, A. L. (2001) Atrogin-1, a muscle-specific F-box protein highly expressed during muscle atrophy. *Proceedings of the National Academy of Sciences of the United States of America* **98**, 14440-14445

6. Cosper, P. F., and Leinwand, L. A. (2012) Myosin heavy chain is not selectively decreased in murine cancer cachexia. *International journal of cancer* **130**, 2722-2727

7. Ciciliot, S., Rossi, A. C., Dyar, K. A., Blaauw, B., and Schiaffino, S. (2013) Muscle type and fiber type specificity in muscle wasting. *The international journal of biochemistry & cell biology* **45**, 2191-2199

8. Constantinou, C., Fontes de Oliveira, C. C., Mintzopoulos, D., Busquets, S., He, J., Kesarwani, M., Mindrinos, M., Rahme, L. G., Argiles, J. M., and Tzika, A. A. (2011) Nuclear magnetic resonance in conjunction with functional genomics suggests mitochondrial dysfunction in a murine model of cancer cachexia. *International journal of molecular medicine* **27**, 15-24
9. McLean, J. B., Moylan, J. S., and Andrade, F. H. (2014) Mitochondria dysfunction in lung cancer-induced muscle wasting in C2C12 myotubes. *Frontiers in physiology* **5**, 503

10. Scatena, R. (2012) Mitochondria and cancer: a growing role in apoptosis, cancer cell metabolism and dedifferentiation. in *Advances in Mitochondrial Medicine*, Springer. pp 287-308

11. Giordano, A., Calvani, M., Petillo, O., Carteni, M., Melone, M. R., and Peluso, G. (2003) Skeletal muscle metabolism in physiology and in cancer disease. *Journal of cellular biochemistry* **90**, 170-186

12. Jemal, A., Bray, F., Center, M. M., Ferlay, J., Ward, E., and Forman, D. (2011) Global cancer statistics. *CA: a cancer journal for clinicians* **61**, 69-90

13. Fearon, K. C. (2008) Cancer cachexia: developing multimodal therapy for a multidimensional problem. *European journal of cancer* **44**, 1124-1132

14. Ice, R. J., McLaughlin, S. L., Livengood, R. H., Culp, M. V., Eddy, E. R., Ivanov, A. V., and Pugacheva, E. N. (2013) NEDD9 depletion destabilizes Aurora A kinase and heightens the efficacy of Aurora A inhibitors: implications for treatment of metastatic solid tumors. *Cancer research* **73**, 3168-3180

15. Pistilli, E. E., Jackson, J. R., and Alway, S. E. (2006) Death receptor-associated pro-apoptotic signaling in aged skeletal muscle. *Apoptosis : an international journal on programmed cell death* **11**, 2115-2126

16. Aulino, P., Berardi, E., Cardillo, V. M., Rizzuto, E., Perniconi, B., Ramina, C., Padula, F., Spugnini, E. P., Baldi, A., and Faiola, F. (2010) Molecular, cellular and physiological characterization of the cancer cachexia-inducing C26 colon carcinoma in mouse. *BMC cancer* **10**, 363

17. Roberts, B., Frye, G., Ahn, B., Ferreira, L., and Judge, A. (2013) Cancer cachexia decreases specific force and accelerates fatigue in limb muscle. *Biochemical and biophysical research communications* **435**, 488-492

18. Fearon, K. C., Glass, D. J., and Guttridge, D. C. (2012) Cancer cachexia: mediators, signaling, and metabolic pathways. *Cell metabolism* **16**, 153-166

19. Acharyya, S., Butchbach, M. E., Sahenk, Z., Wang, H., Saji, M., Carathers, M., Ringel, M. D., Skipworth, R. J., Fearon, K. C., Hollingsworth, M. A., Muscarella, P., Burghes, A. H., Rafael-Fortney, J. A., and Guttridge, D. C. (2005) Dystrophin glycoprotein complex dysfunction: a regulatory link between muscular dystrophy and cancer cachexia. *Cancer cell* **8**, 421-432

20. Pistilli, E. E., Bogdanovich, S., Garton, F., Yang, N., Gulbin, J. P., Conner, J. D., Anderson, B. G., Quinn, L. S., North, K., Ahima, R. S., and Khurana, T. S. (2011) Loss of IL-15 receptor alpha alters the endurance, fatigability, and metabolic characteristics of mouse fast skeletal muscles. *The Journal of clinical investigation* **121**, 3120-3132

21. EWENS, A., MIHICH, E., and EHRKE, M. J. (2005) Distant metastasis from subcutaneously grown E0771 medullary breast adenocarcinoma. Anticancer research 25, 3905-3915

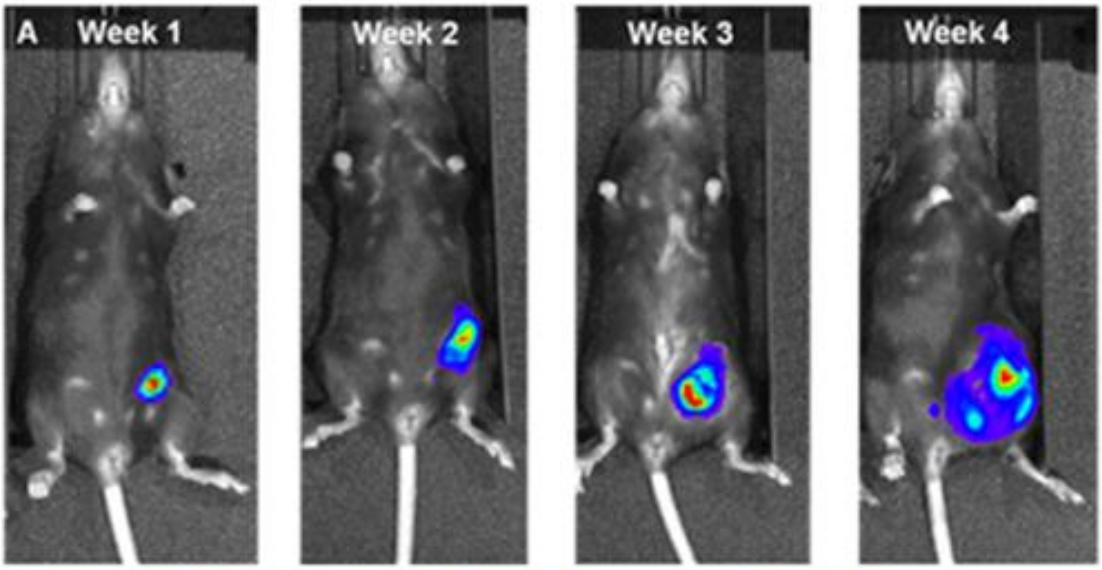

Figure 1 IVIS Imaging of C57BL6 mouse: Weekly measurements were taken by injecting mice with luciferin and measuring fluoresce. The EO771 cell line produced a solid tumor and increased in flux each week.

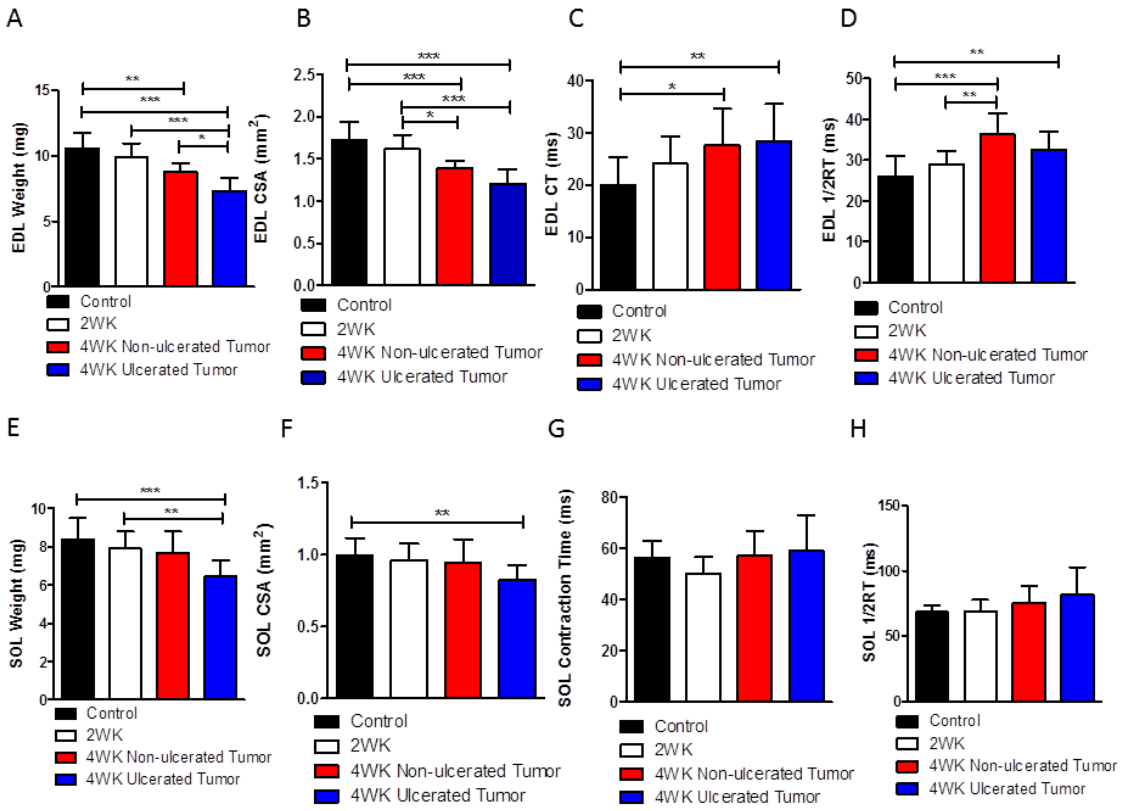

Figure 2

EDL and SOL WT, CSA, CT and ½ RT: A, B. EDL weight (mg) and CSA (mm^2) showed significant decreases in the 4 WK Ulcerated Tumor group. E, F. EDL CT and ½ RT showed significant increases hinting at alterations in Calcium handling during contractions. C, D. SOL weight (mg) and CSA (mm2) showed significant decreases in the 4 WK Ulcerated Tumor group. G, F. No differences were seen in SOL CT and ½ RT. CON (n=8), 2WK (n=5), 4WK Non (n=4), 4WK Ulc (n=5). *=P<0.05, **=P<0.005, ***=P<0.0001

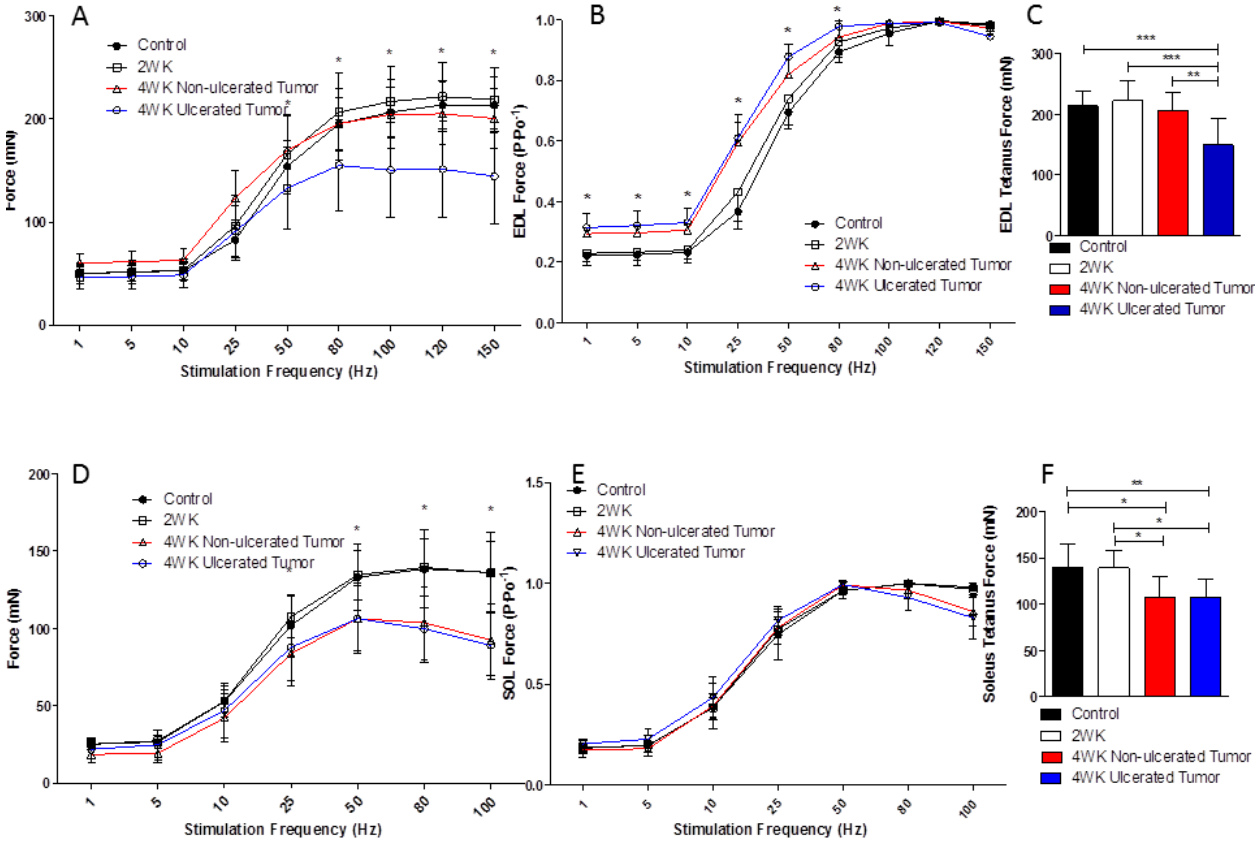

Figure 3

EDL and SOL Force Frequency and Tetanus. A, B**.** EDL Absolute and Relative Force Frequency showed a shift similar to a oxidative muscle phenotype in both 4WK groups indicating a decrease in absolute force output and force output relative to maximal contraction showing EDL muscle producing higher forces at earlier stimulation frequencies. E. 4WK Ulcerated Tumor EDL Max Tetanus showed a significant decrease in force (mN) when compared to other groups. C, D. Both 4WK groups showed a shift in the Absolute Force Frequency however, Relative Force Frequency showed no differences. F. SOL Max Tetanus showed a significant decrease in both 4WK tumor groups. CON (n=8), 2WK (n=5), 4WK Non (n=4), 4WK Ulc (n=5). *=P<0.05, **=P<0.005, ***=P<0.0001

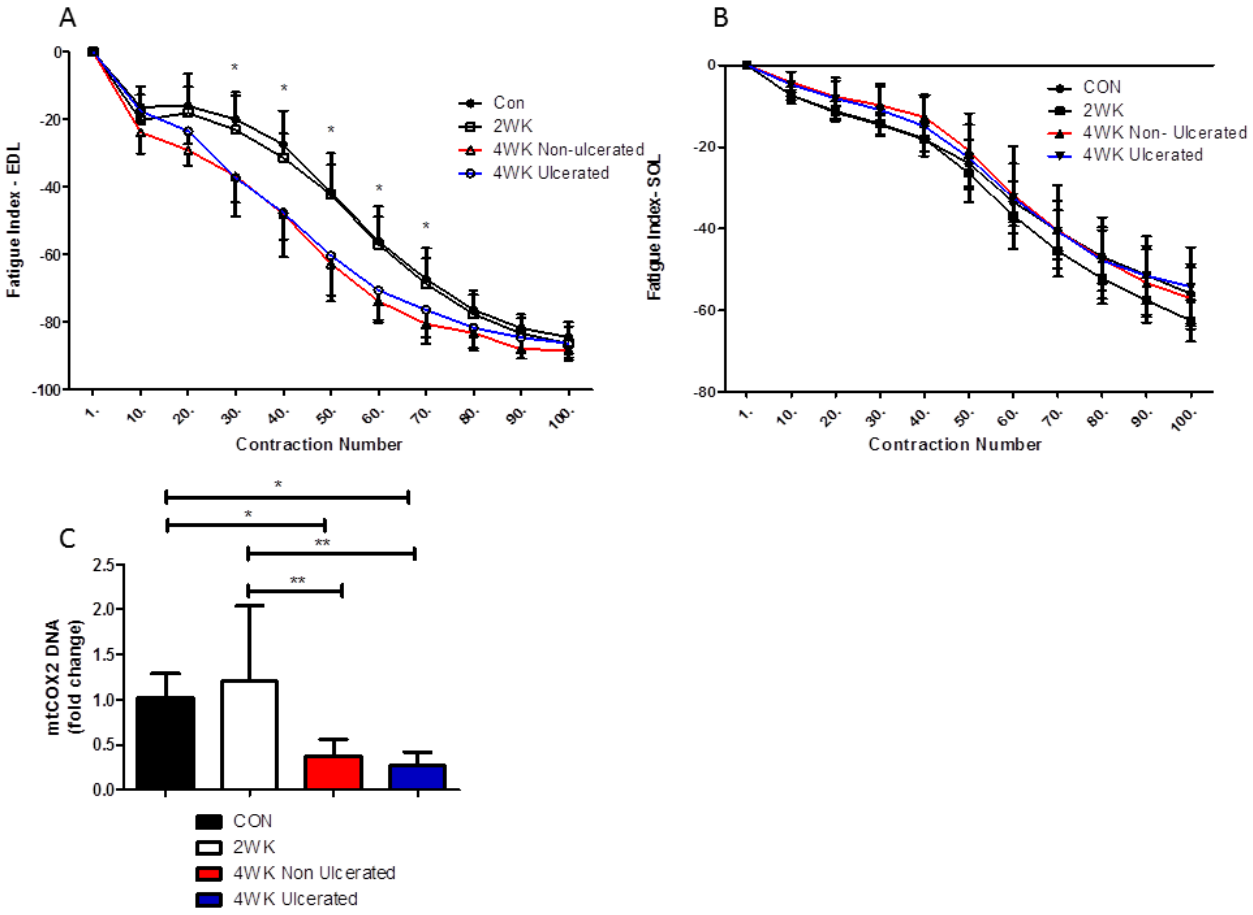

Figure 4

EDL and SOL Fatigue curve, Mitochondria DNA Content. A. Both 4WK Tumor bearing groups showed a significant increase in fatigue shifting down and to the left. 2WK mice remain un-affected when compared to CON B. No Differences were found in SOL Fatigue across all groups. C. Mitochondrial DNA Content showed a significant reduction in content in both 4WK groups, coinciding with the shift in the fatigue curve in A. CON (n=8), 2WK (n=5), 4WK Non (n=4), 4WK Ulc (n=5). *=P<0.05, **=P<0.005, ***=P<0.0001

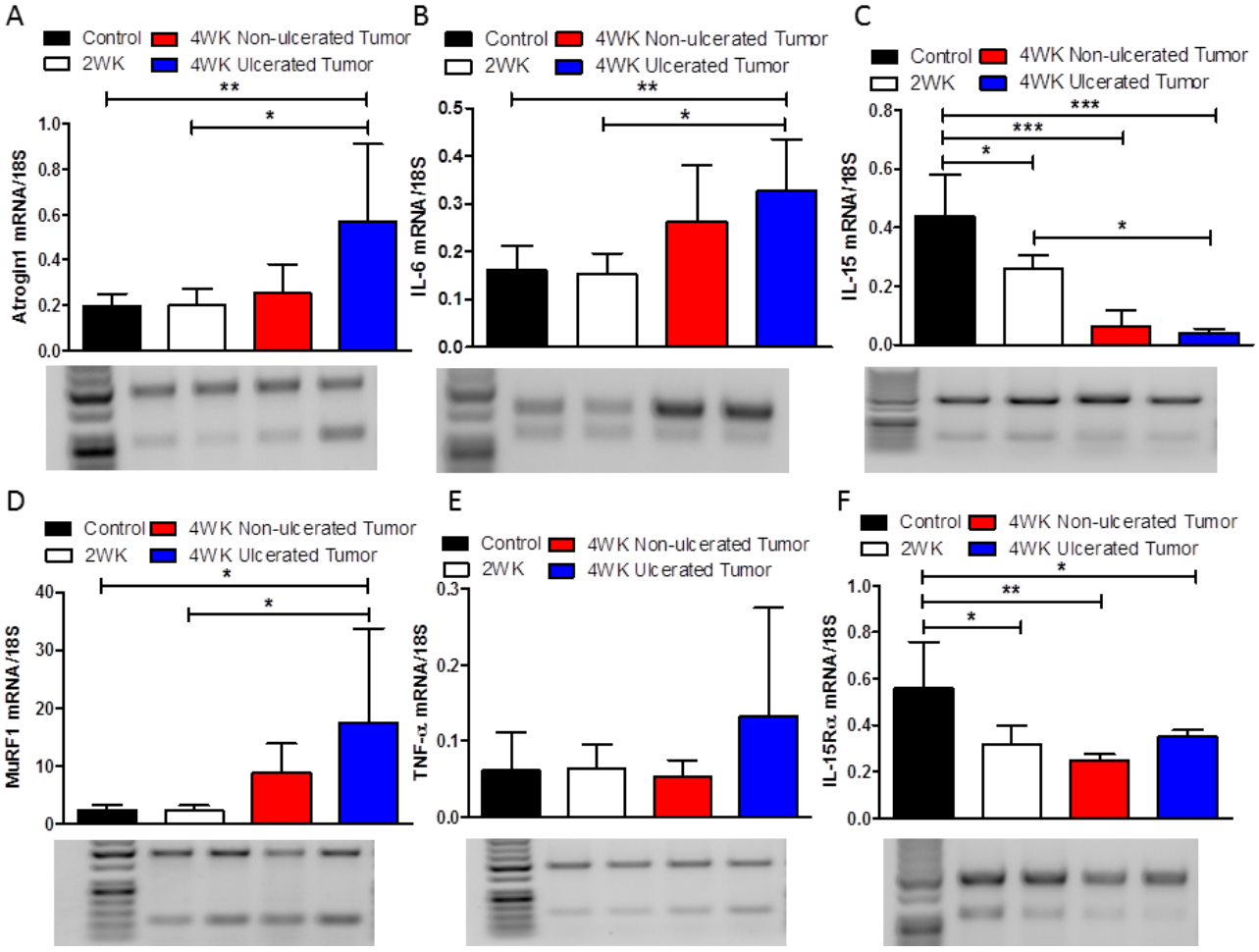

Figure 5

RNA Isolation from Tibialus Anterior muscles: All groups represented as Con/2WK/4WK NUT/4WK UT A. PCR amplification of Atrogin1 revealed significantly higher levels in the 4WK UT group compared to CON. B. PCR amplification of IL-6 revealed significantly higher levels in the 4WK UT group compared to CON C. PCR amplification of IL-15 showed significant decreases in both 4WK groups when compared to CON and 2WK groups. D. PCR amplification of Murf1 showed significant increase in the 4WK UT group when compared to CON. E. PCR amplification of TNF-α showed a modest trend towards increasing in the 4WK UT group, however significance was not reached. F. PCR amplification of IL-15 rα showed significant decreases in all 3 tumor bearing groups when compared to CON. CON (n=8), 2WK (n=5), 4WK Non (n=4), 4WK Ulc (n=5). *=P<0.05, **=P<0.005, ***=P<0.0001

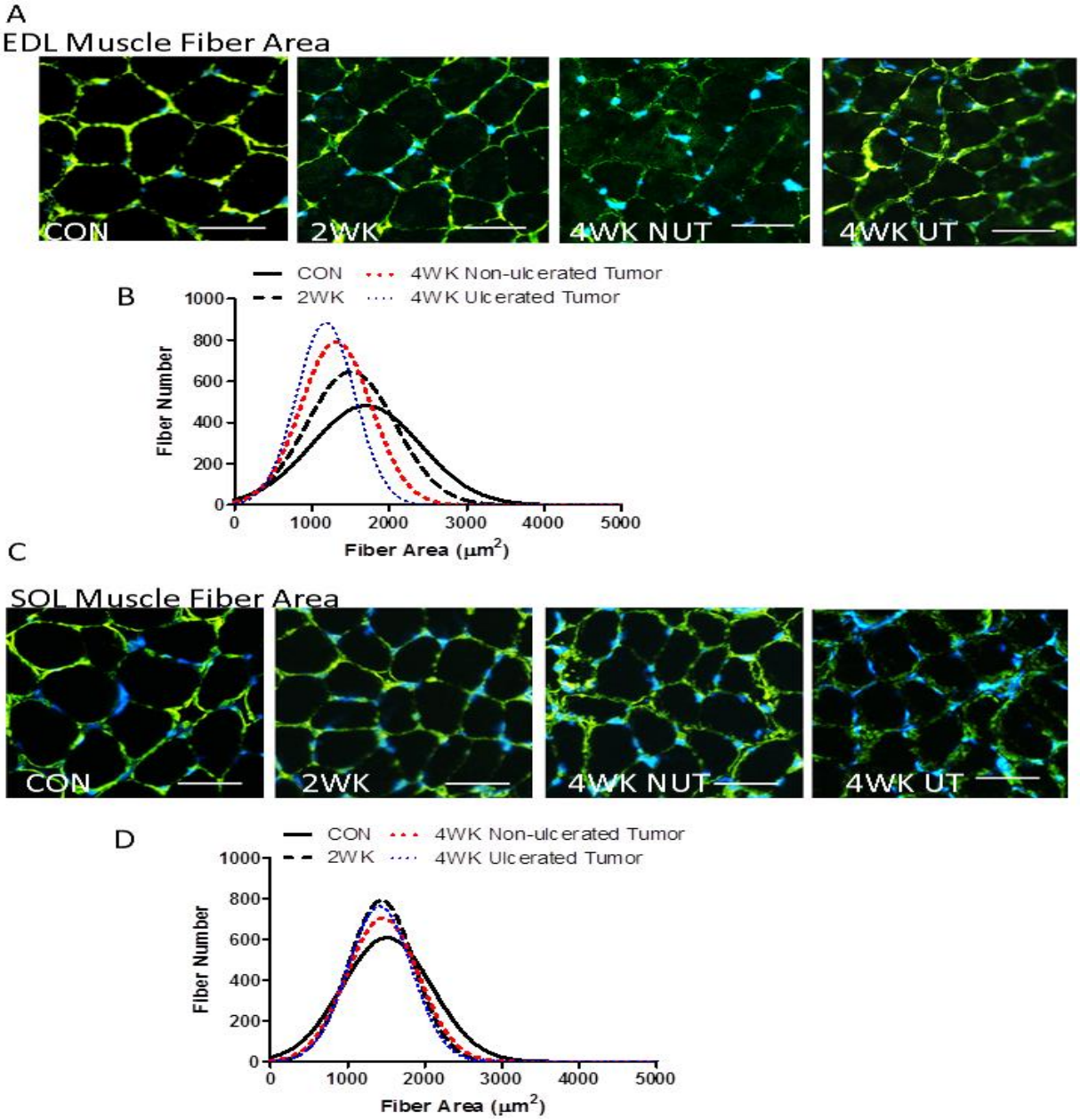

Figure 6

EDL and SOL Muscle Fiber Area: A. From Left to Right CON, 2WK, 4WK Non-Ulcerated, 4WK Ulcerated. B. EDL Muscles show a shift in the Fiber Number with progression of cancer, with a larger culmination of smaller fibers in the 4WK Ulcerated group. C. The EDL Cumulative Frequency shows a shift to the right indicating similar results as B., D. From Left to Right CON, 2WK, 4WK Non-Ulcerated, 4WK Ulcerated. E, F. Fiber number and Cumulative Frequency show no real differences between groups. CON (n=4), 2WK (n=4), 4WK Non (n=4), 4WK Ulcerated (n=4)

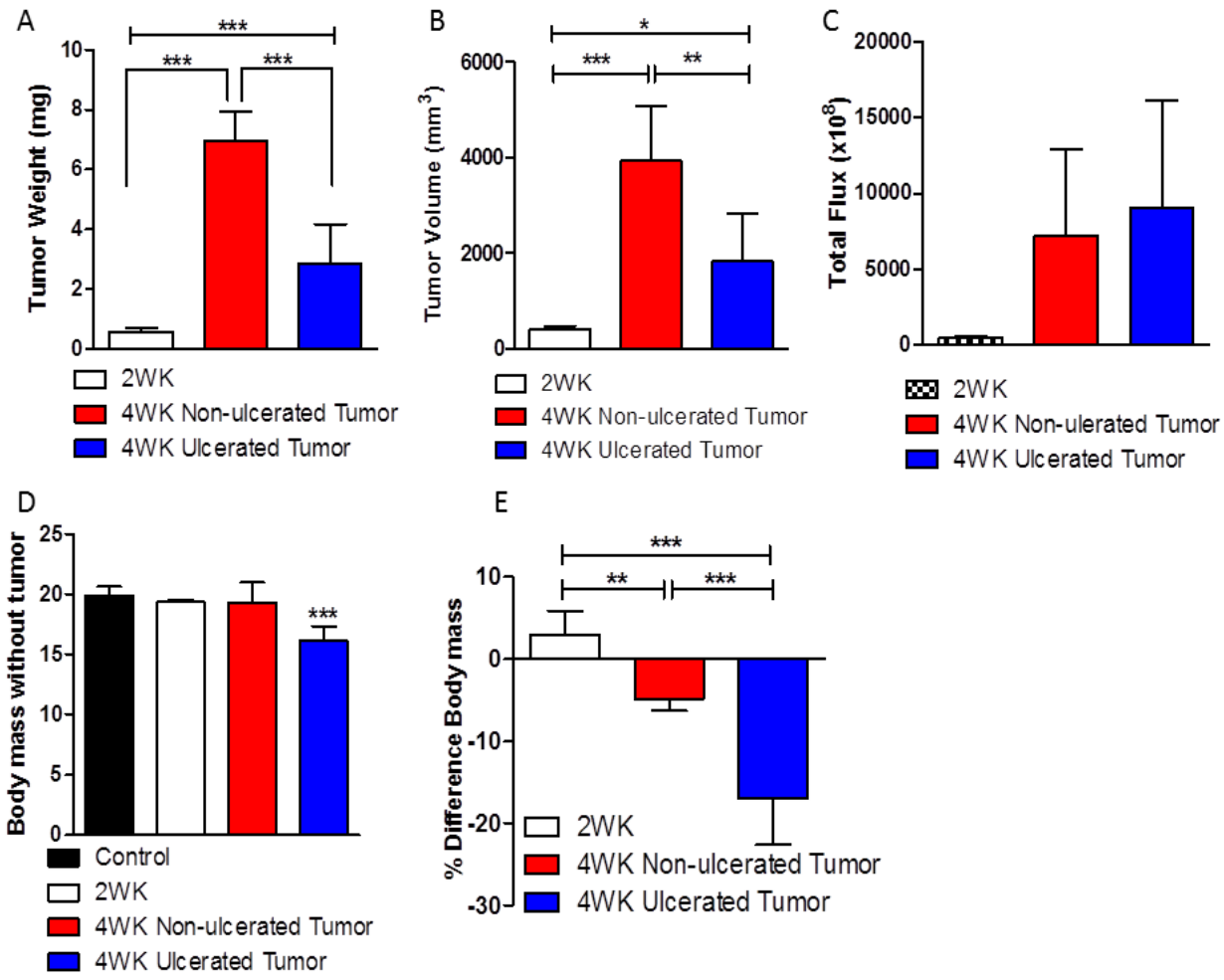

Figure 7

Tumor Weight/Volume and Body Weight: A Tumor Weight of the 3 tumor bearing groups (mg). 4WK Non-ulcerated Tumors weight the most and was significantly greater then both 2WK and 4WK Ulcerated. B. Tumor Volume (mm^3) in 3 tumor groups. Similar to weight, 4WK Non-ulcerated tumors had the largest volume compared to 2WK and 4WK ulcerated. C Tumor Flux ($x10^8$) in 3 tumor groups. Both 4WK groups had a similar trend of a larger tumor flux. D. Body mass after removal of the tumor (mg). 4WK Ulcerated Tumor mice had a significant decrease in body mass. E % Difference in Body Mass. 4WK Ulcerated Mice had the largest difference in body mass when comparing pre-injection of cells and post-dissection CON (n=8), 2WK (n=5), 4WK Non (n=4), 4WK Ulc (n=5). *=P<0.05, **=P<0.005, ***=P<0.0001

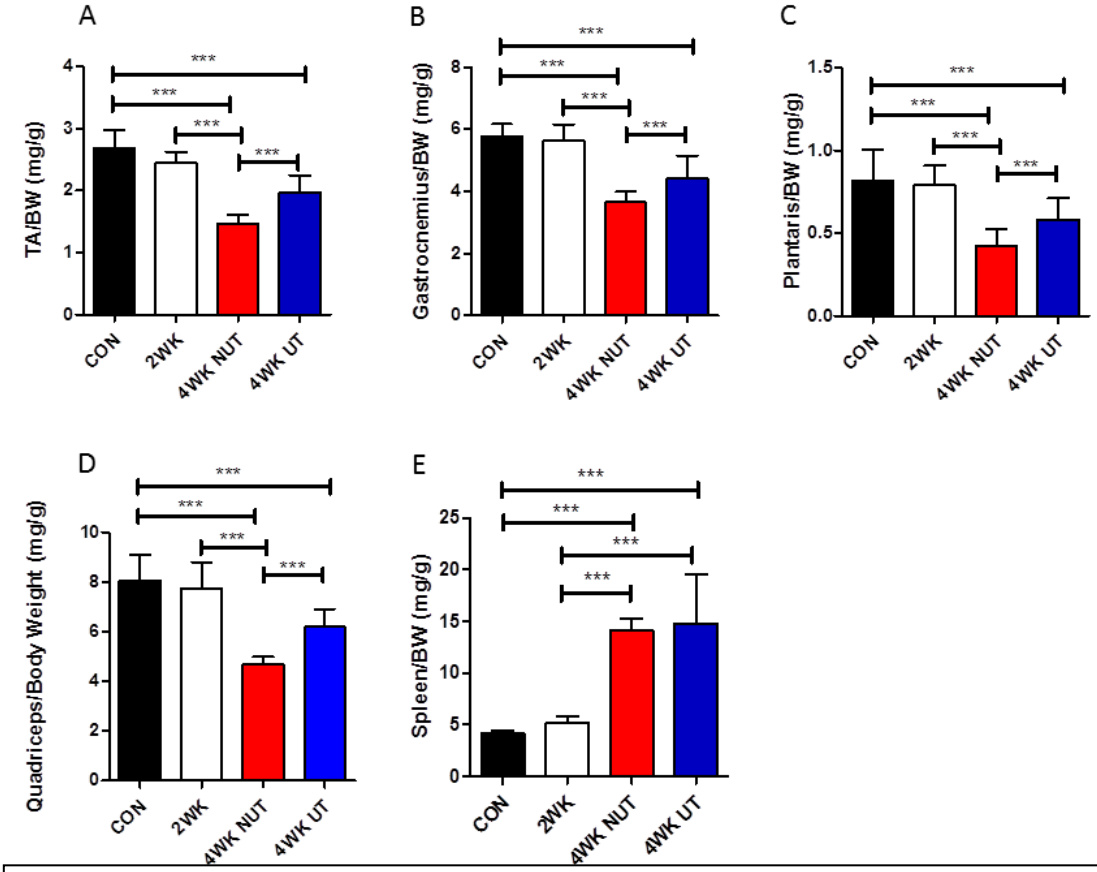

Figure 8 Muscle and Spleen Normalized BW: A. Tibialus Anterior weight normalized to body weight. B. Gastrocnemius weight normalized to body weight. C. Plantaris weight normalized to body weight. D. Quadriceps muscle normalized to body weight. E. Spleen weight normalized to body weight. CON (n=8), 2WK (n=5), 4WK Non (n=4), 4WK Ulc (n=5). *=P<0.05, **=P<0.005, ***=P<0.0001

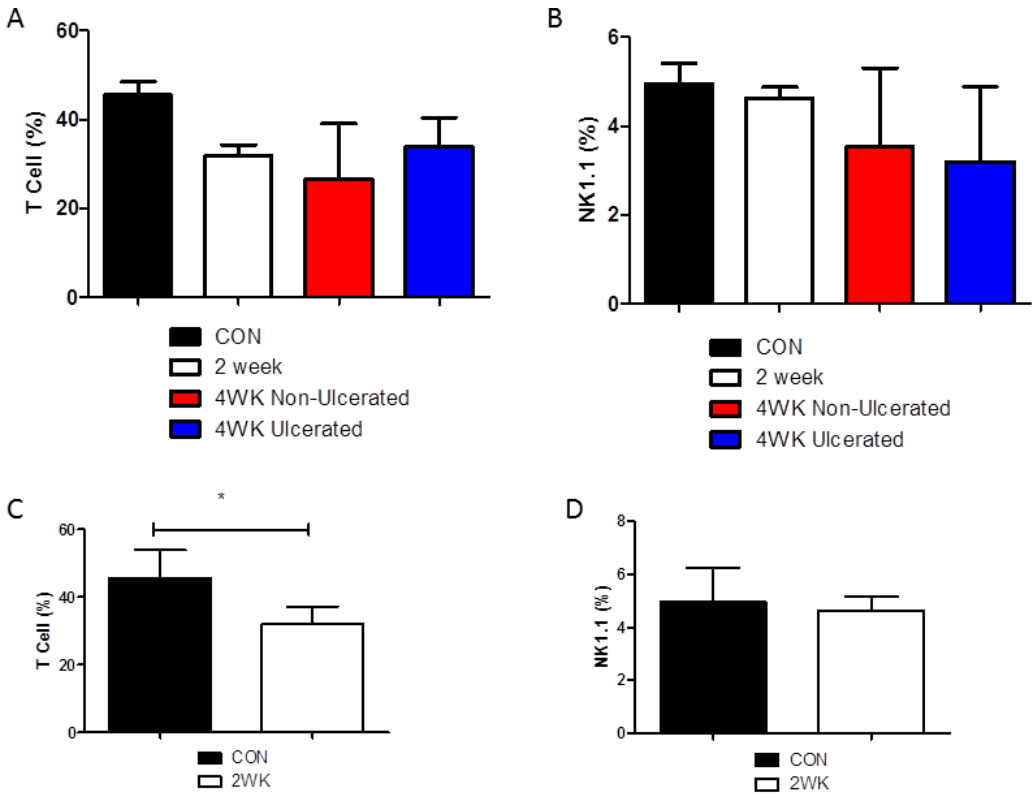

Figure 9 Spleen T Cell and NK Cell %: A., B. No differences were seen between groups with regards to T Cell or NK Cell. C. T Cell comparison of CON and 2WK time points shows a significant decrease at 2 weeks. D. No differences in CON vs 2WK time points. . CON (n=8), 2WK (n=5), 4WK Non (n=4), 4WK Ulc (n=5). *=P<0.05

Chapter 4

Results: IL-15 Overexpression in Transgenic Mice

4.1

Effects of IL-15 Skeletal Muscle Overexpression on Muscle WT, CSA, CT and ½RT

In order to test the effects of cancer cachexia on skeletal muscle function we purchased the IL-15 Skeletal Muscle overexpressor mouse from Jackson Laboratory. These mice have previously been characterized by Quinn (52). In brief, the HSA-IL2SP-IL15 construct uses a Human alpha-skeletal actin promoter region, along with an IL-2 signal peptide region combine with Murine IL-15 cDNA. This construct yields

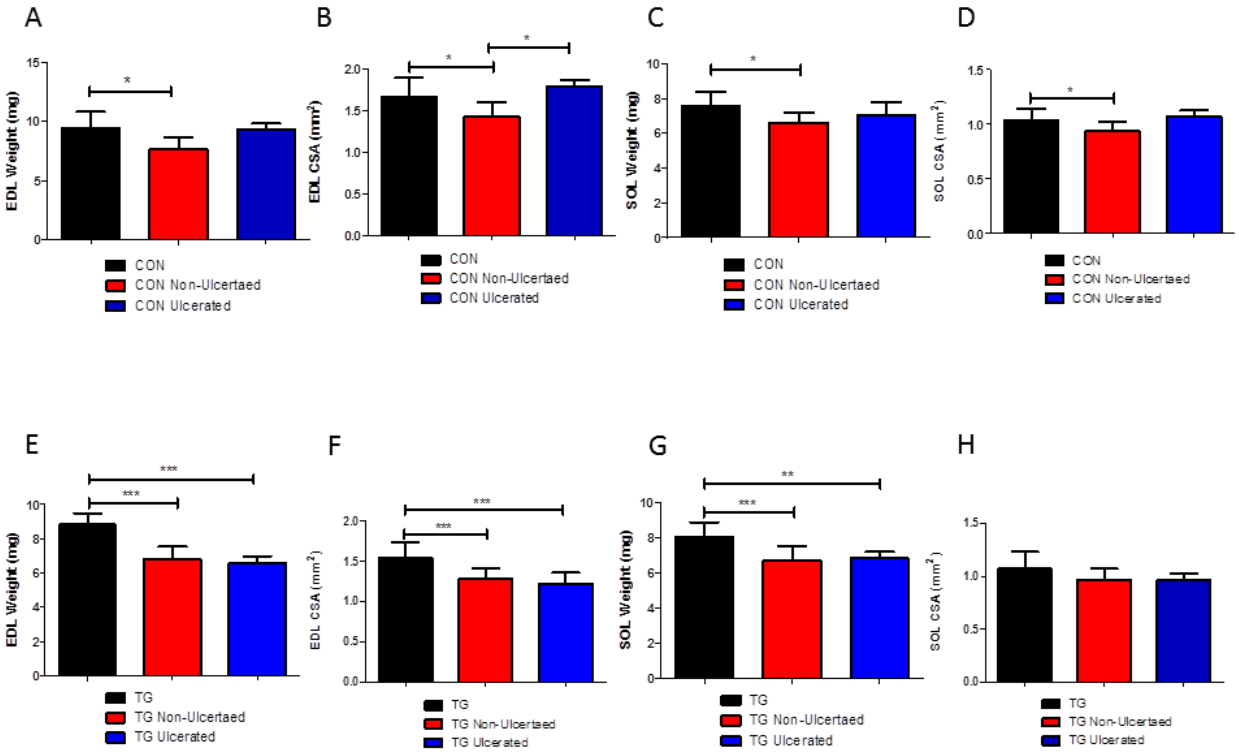

Figure 10 EDL/SOL Weight and CSA: A., C. CON EDL/SOL Weights with a significant decrease with the CON Non-Ulcerated group. B., D. CON EDL/SOL CSA with a significant decrease with the CON Non-Ulcerated group E., G. TG EDL/SOL Weights showing a significant decrease in both the TG Non-Ulcerated and Ulcerated groups. F. EDL CSA show a significant decrease in both the TG Non-Ulcerated and Ulcerated groups. H. No statistical differences were seen between groups for SOL CSA. CON (n=8), CON Non (n=8), CON Ulc (n=2), TG (n=7), TG Non (n=8), TG Ulc (n=4) *=P<0.05, **=P<0.005, ***=P<0.0001

significant increases in skeletal muscle IL-15 mRNA and protein content, as well as increased serum levels of IL-15. (52) Mice were bred yielding both IL-15 skeletal muscle overexpressors (IL-15 TG) and littermate controls (CON). EO771 cells were cultured and injected into the fat pad adjacent to the 4th nipple. For comparison purposes mice were grouped into 6 groups; CON (n=8, un-injected), CON Non-Ulcerated (n=8, injected), CON Ulcerated (n=2, injected), TG (n=7, un-injected), TG Non-Ulcerated (n=7, injected) and TG Ulcerated (n=4, injected).

With regards to the CON groups, EDL and SOL weights was shown to

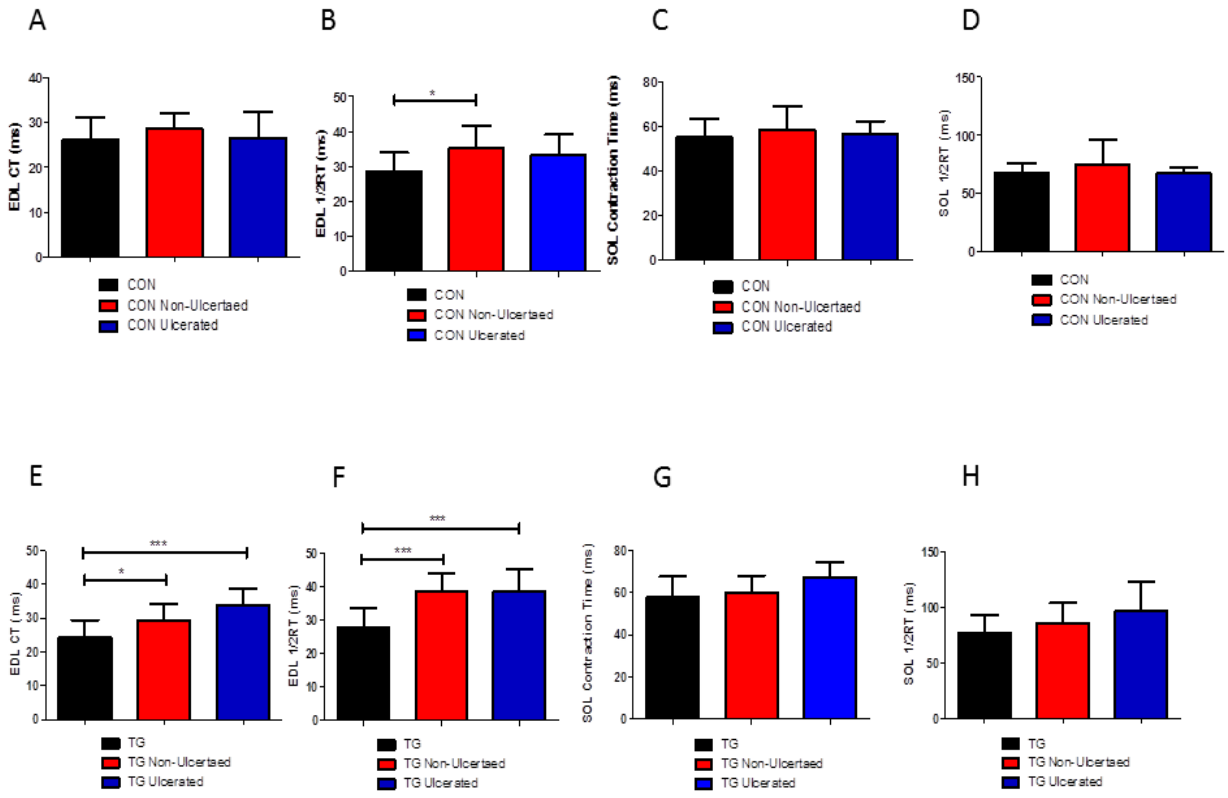

Figure 11 EDL/SOL CT and ½ RT for CON and TG: A. EDL CT showed no differences between groups. B. EDL ½ RT showed significant increases in the CON Non-Ulcerated group. C., D. SOL CT and ½ RT showed not differences in the CON groups. E., F. EDL muscles showed a significant increase in CT and ½ RT in both the TG Non-Ulcerated and TG Ulcerated Group. G., H. SOL muscles showed no differences between groups in both CT and ½ RT. CON (n=8), CON Non (n=8), CON Ulc (n=2), TG (n=7), TG Non (n=8), TG Ulc (n=4) *=P<0.05, **=P<0.005. ***=P<0.0001

significantly decrease with the CON Non-Ulcerated Tumor group (Figure 10A, 10C). While the CON Ulcerated groups did not reach significance, it is important to note this group had 2 mice perhaps showing why significance was not reached in this or any of the subsequent groups. CSA for both EDL and SOL showed a significant decrease with the CON Non-Ulcerated Tumor group (Figure 10B, 10D). The TG group showed a significant decrease in the EDL and SOL weights in both the TG Non-Ulcerated and

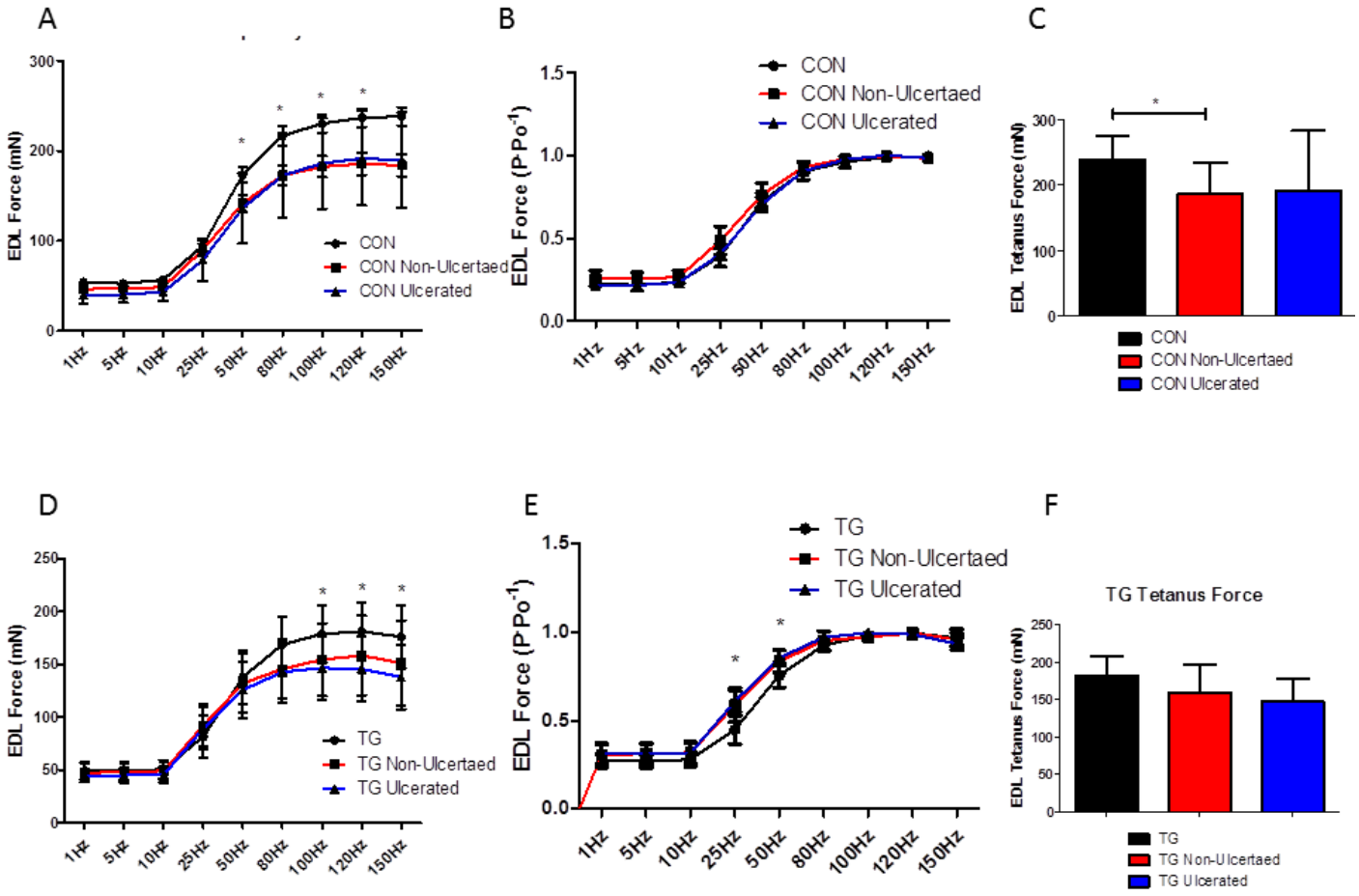

Figure 12 EDL Relative and Absolute Force Frequency: A. EDL Absolute Force frequency shows a significant reduction in tetanus force in the 50-150Hz stimulation frequency's for the CON Non-Ulcerated and CON Ulcerated. B. EDL Relative Force Frequency shows no significant difference between groups. C. EDL Maximal Tetanus was significantly reduced in the CON Non-Ulcerated group. D. EDL Absolute Force Frequency showed a significant reduction in the 100-150Hz stimulation frequency's for the TG Non-Ulcerated and TG Ulcerated groups. E. Relative Force Frequency showed a small shift in the 25-50Hz stimulation frequency's for the TG Non-Ulcerated and TG Ulcerated groups. F. No statistical differences were seen for maximal tetanus force for the TG groups. CON (n=8), CON Non (n=8), CON Ulc (n=2), TG (n=7), TG Non (n=8), TG Ulc (n=4) *=P<0.05, **=P<0.005, ***=P<0.0001

Ulcerated groups (Figure 10E, 10G). EDL CSA was shown to significantly decrease in the TG Non-Ulcerated and Ulcerated groups (Figure 10F) with no effect on SOL CSA (Figure 10H). Overall we see a similar trend with muscle weights and CSA to the preliminary study in B6 mice.

No differences were seen between CON, CON Non-Ulcerated and CON Ulcerated with regards to EDL CT, SOL CT and SOL ½ RT (Figure 10A, 10C, 10D).

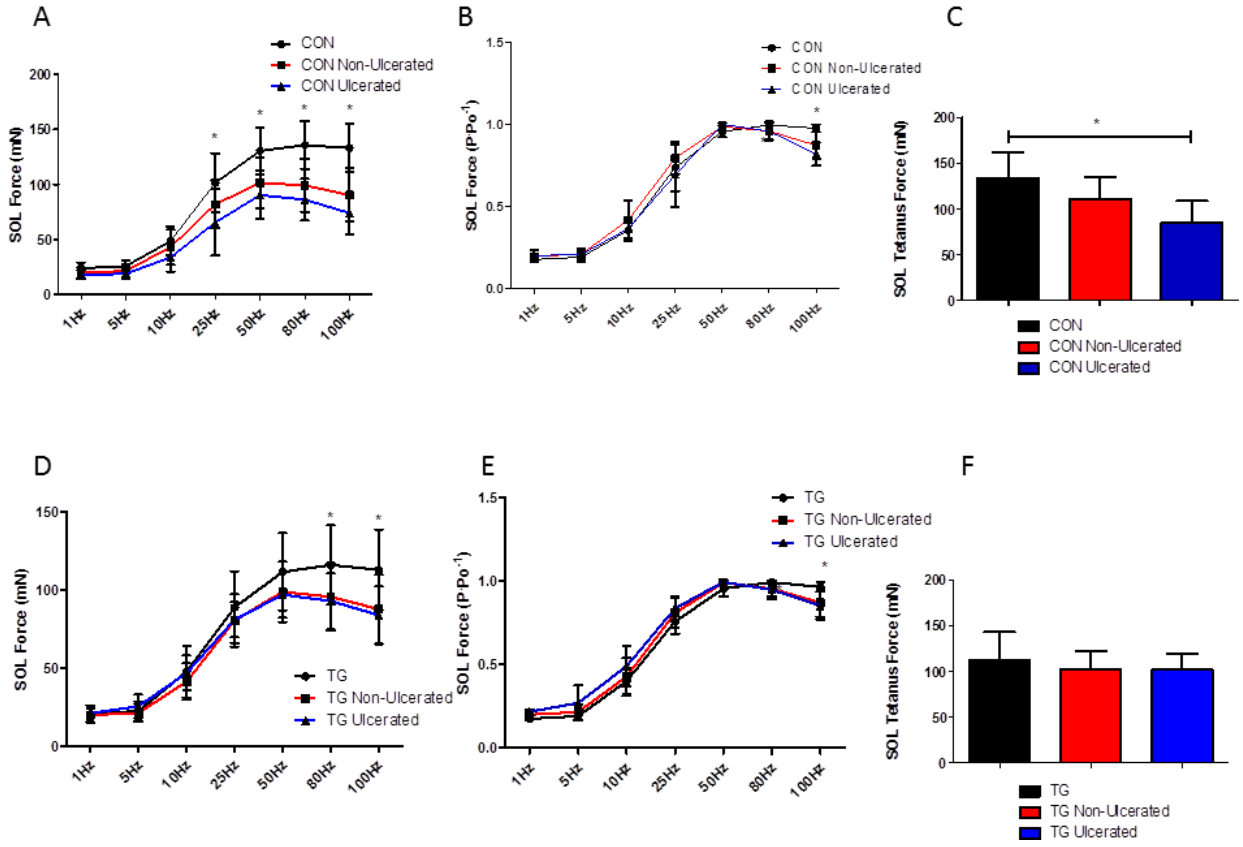

Figure 13 SOL Relative and Absolute Force Frequency: A. Sol Absolute Force Frequency showed a significant decrease in both the CON Non-Ulcerated and CON Ulcerated group compared to the CON group at the 25Hz-100Hz stimulation frequency. B. Relative Force Frequency show a significant shift at the 100Hz stimulation frequency in both the CON Non-Ulcerated and CON Ulcerated groups. C. SOL Maximal Tetanus force showed a significant decrease in the CON Ulcerated group when compared to the CON group. D. SOL Absolute Force Frequency showed a significant decrease in both the TG Non-Ulcerated and TG Ulcerated groups at the 80Hz-100Hz stimulation frequency. E. SOL Relative Force Frequency a significant shift at the 100Hz stimulation in both the TG Non-Ulcerated and TG Ulcerated groups. F. SOL Maximal Tetanus Force showed no statistical difference between groups. CON (n=8), CON Non (n=8), 4WK Ulc (n=2), TG (n=7), TG Non (n=8), TG Ulc (n=4) *=P<0.05, **=P<0.005, ***=P<0.0001

EDL ½ RT did show a significant increase in the CON Non-Ulcerated groups. In the TG groups, EDL CT and ½ RT both showed significant increases in the TG Non-Ulcerated and TG Ulcerated group (Figure 11E, 11F). The SOL muscle showed no differences in either CT or ½ RT. (Figure 11G, 11H).

3.6

Effects of IL-15 Skeletal Muscle Overexpression on Tetanic Force and Muscle Fatigue

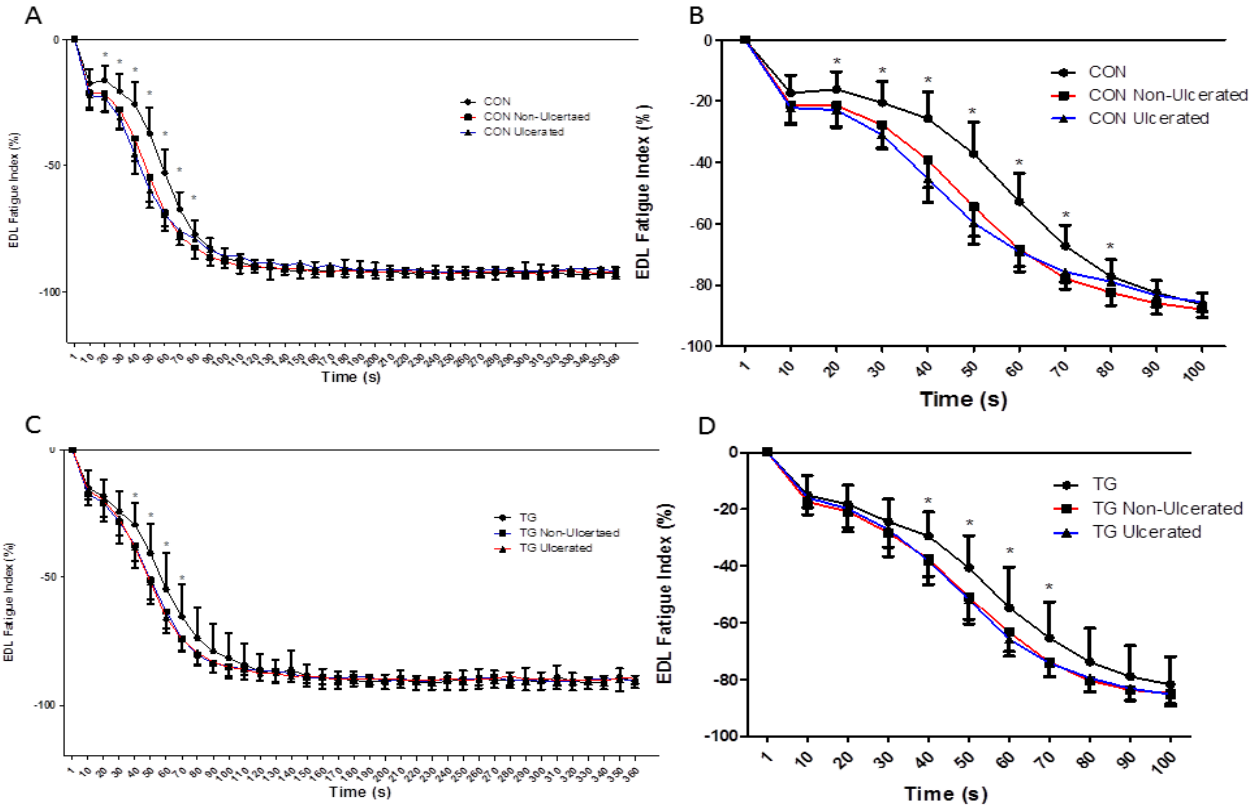

Figure 14 EDL Fatigue Curve for CON and TG: A. EDL fatigue curve showing a significant shift in both the CON Non-Ulcerated and CON Ulcerated groups for the 20-80 second time points. B. EDL fatigue tracing of the first 100 seconds. C. EDL fatigue curve shows a significant shift in both the TG Non-Ulcerated and TG Ulcerated groups for the 40-70 second time points. D. EDL fatigue tracing of the first 100 seconds. CON (n=8), CON Non (n=8), CON Ulc (n=2), TG (n=7), TG Non (n=8), TG Ulc (n=4) *=P<0.05, **=P<0.005, ***=P<0.0001

EDL absolute force in the control group yielded a significant reduction of force production in the CON Non-Ulcerated and CON Ulcerated indicating a weaker muscle in the presence of cancer (Figure 12 A). When looking at relative force however we see no shifts in the force curve, indicating these forces are producing normal tetanus for their relative frequency of stimulation (Figure 12 B). EDL tetanus force did see a significant decrease in the CON Non-Ulcerated group (Figure 12 C). These results may

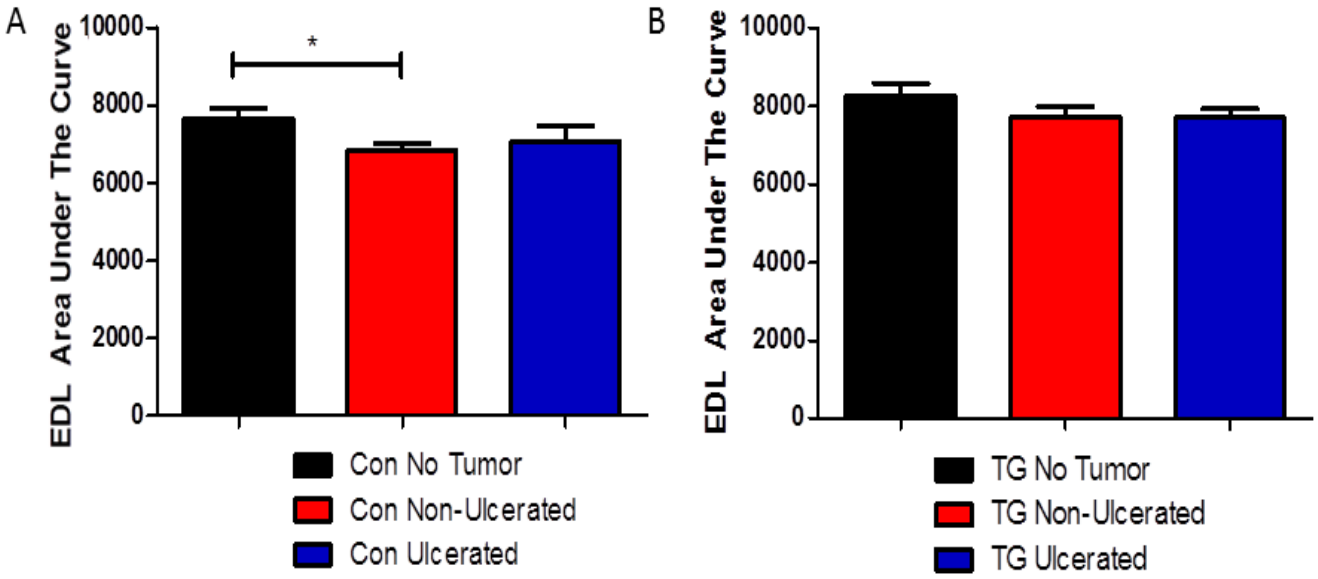

Figure 15 EDL Area Under the Fatigue Curve A. EDL Total Area Under the Fatigue Curve showed a significant reduction in the Con Non-Ulcerated group compared to CON. B. No statistical differences were seen between TG groups. CON (n=8), 4WK Non (n=8), 4WK Ulc (n=2), TG (n=7), TG Non (n=8), 4WK (n=4) *=P<0.05, **=P<0.005, ***=P<0.0001

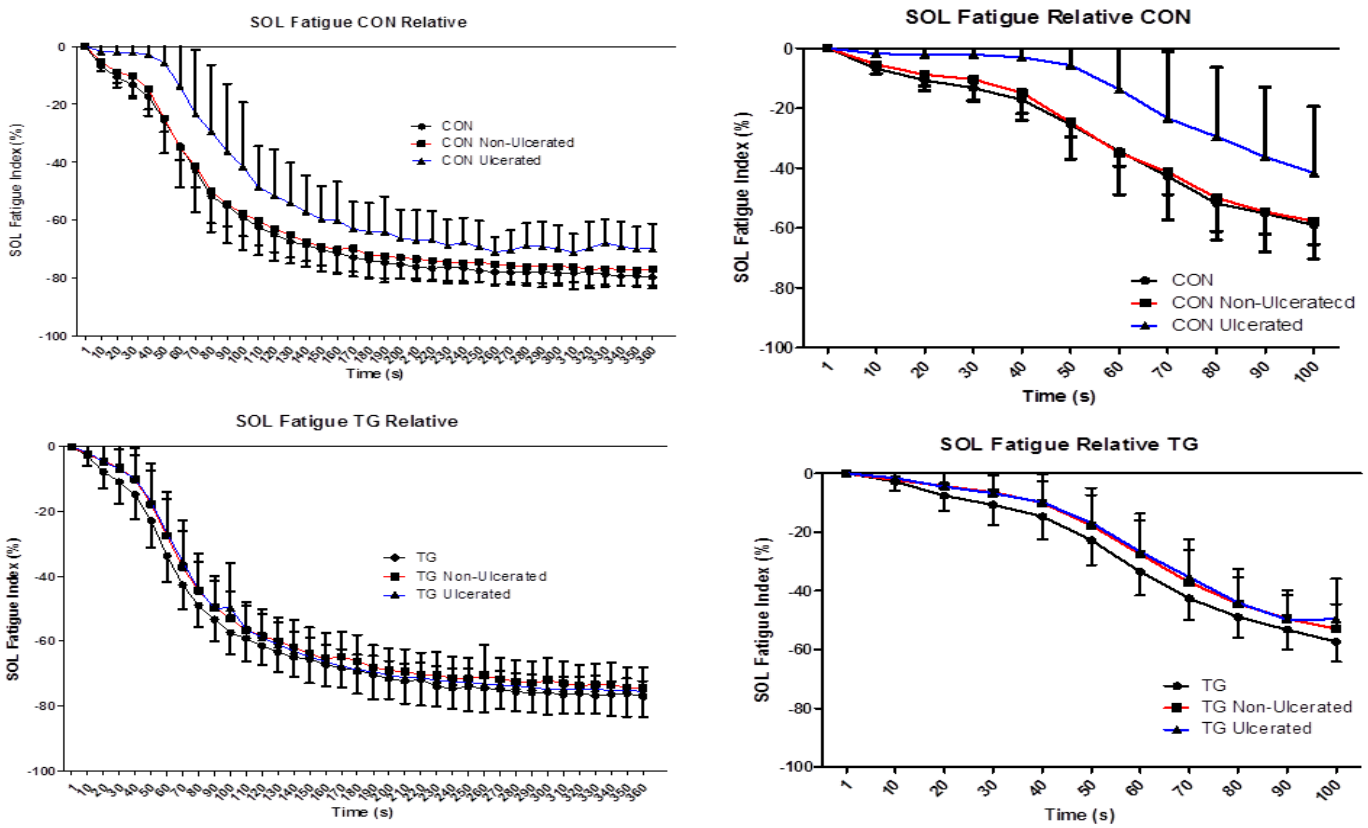

Figure 16 SOL Fatigue Curve for CON and TG: A. SOL fatigue curve showing a significant shift in in both the CON and the CON Ulcerated group compared to the CON Non-Ulcerated group. B. SOL fatigue tracing of the first 100 seconds. C. SOL fatigue curve showing no statistical differences between groups. D. SOL fatigue tracing of the first 100 seconds. CON (n=8), CON Non (n=8), CON Ulc (n=2), TG (n=7), TG Non (n=8), TG Ulc (n=4) *=P<0.05, **=P<0.005, ***=P<0.0001

change when boosting the CON Ulcerated group. EDL Absolute Tetanus Force in the TG groups saw a significant reduction in the TG Non-Ulcerated and TG Ulcerated groups compared to control (Figure 12 D). When looking at relative Tetanus there is a slight significant shift at the 25-50Hz points for the TG Non-Ulcerate and TG Ulcerated (Figure 12 E). EDL max tetanus however, shows no significant differences between the groups of TG mice (Figure 12 F). SOL muscles in the control group yielded a significant decrease in absolute force frequency in the CON Non-Ulcerated and CON Ulcerated group when compared to the CON group at the 25Hz-100Hz stimulation frequency (Figure 13A). Relative force frequency however, showed only a significant shift at the 100Hz stimulation frequency CON Non-Ulcerated group and CON Ulcerated group

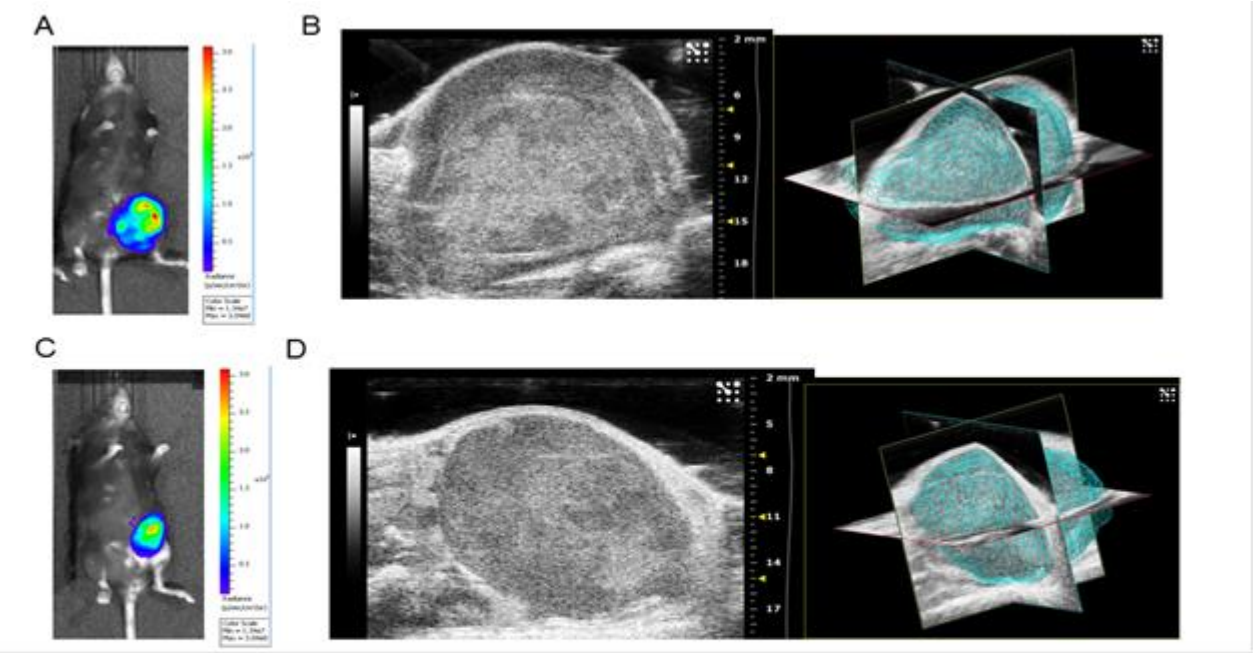

Figure 17 IVIS Imaging and In Vevo Ultrasound of Tumors from CON and TG Mice: A. Visual representation of IVIS Imaging of CON mice measured in radiance (p/sec/cm^2/sr). B. Cross section of largest area of tumor as well as a 3D model of CON tumor. C. Visual representation of IVIS Imaging of TG mice measured in radiance (p/sec/cm^2/sr). D. Cross section of largest area of tumor as well as a 3D model of CON tumor.

when comparing to the CON group (Figure 13B). Interestingly, the CON Ulcerated group produced significantly less maximal tetanic force when compared to the CON group (Figure 13 C). Transgenic SOL muscles showed a significant decrease in absolute force in both the TG Non-Ulcerated and TG Ulcerated group at the 80Hz-100Hz stimulation frequencies (Figure 13 D). Similar to the CON group, TG mice showed a significant shift in the relative force frequency at the 100Hz stimulation frequency in both the TG Non-Ulcerated and TG Ulcerated (Figure 13 E). TG SOL muscles showed no statistical differences in maximal tetanus force between any of the groups. The EDL fatigue tracing of the CON group showed a significant shift down and to the left in both the CON Non-Ulcerated and CON Ulcerated (20-80 seconds) indicating a significant amount of fatigue in these mice (Figure 14 A) similar to the

tracing seen in the B6 preliminary study (Figure 4 A). EDL fatigue tracing in the TG group showed a significant shift down and to the left in the TG Non-Ulcerated and TG Ulcerated groups (40-70 seconds) however it was a smaller shift in fatigue as well as a smaller duration indicating attenuation of fatigue in the EDL muscle (Figure 14 C). EDL AUC measurements showed a significant reduction in area in the CON Non-Ulcerated group compared to the CON group Figure 15. EDL TG AUC showed no differences between groups. SOL fatigue curves for the CON group show a significant shift down and to the left in the CON and CON Ulcerated group (Figure 16 A). This trend is not typical but perhaps came about because of the small number of mice in the CON

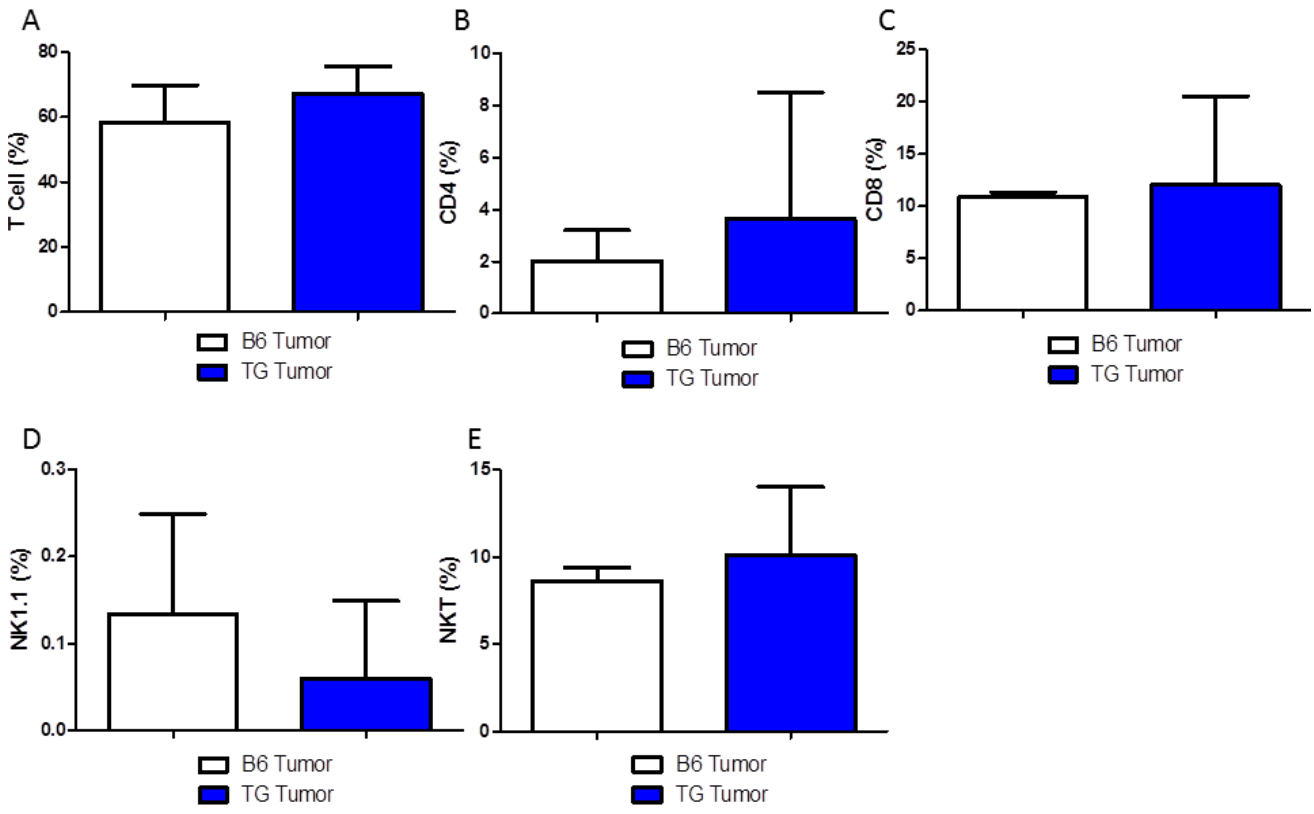

Ulcerated group and the very large SD of the CON Non-Ulcerated group. No

Figure 18 CON and TG Tumor Dissociation: No statistical differences were seen between B6 Tumor and TG Tumor, however there was an overall trend toward increased CD4 (helper) and CD8 (cytotoxic) T cells in the TG mice. CON (n=8), CON Non (n=8), CON Ulc (n=2), TG (n=7), TG Non (n=8), TG Ulc (n=4) *=P<0.05, **=P<0.005, ***=P<0.0001

statistical differences were seen between the TG groups (Figure 16 C).

3.7

IVIS, Ultrasound, Tumor and Spleen cell isolation:

Images were taken every week of both the bioluminescence of each tumor using IVIS imaging as well as the volume of each tumor measured by In Vevo Ultra sound. These data showed no statistical differences in progression of tumor growth when comparing groups. We did see an overall trend towards reduction of tumor size around the 2 week group, however this did not reach significance. After dissecting out whole tumors from mice, single cell suspensions were generated and stained looking for differences in T cell and NK cell populations. No statistical differences were seen between B6 Tumor (n=3) of TG Tumor (n=5), however there was a trend toward increasing in the TG Tumor group which could be further vilified if the groups were increased (Figure 18). When analyzing single cell suspension of the spleen from both CON vs CON Tumor and TG vs TG Tumor we saw a significant reduction in T Cell % in both groups (Figure 19). We did not see any other statistical differences in T Cell or NK Cell populations however in any of the spleen groups. (Figure 19, 20)

3.8

Tumor/Mouse weight, Muscle/BW

No differences were seen between either CON or TG groups with regard to tumor volume or weight (Figure 21 A and B). Body mass was reduced significantly after removal of the tumor in both CON Non-Ulcerated and CON Ulcerated groups, however % change in body mass was not significant (Figure 21 C and D.)

TG Non-Ulcerated mice showed a significant reduction in body mass once the tumor was removed compared to TG uninjected (Figure 21 G). TA/BW showed a significant decrease in both the CON Non-Ulcerated and CON Ulcerated muscles when compared to CON muscles (Figure 22 A). Both the Gastroc/BW and Quad/BW showed significant decreases in the CON Non-Ulcerated when compared to CON muscles (Figure 22 B, D). Only TA/BW showed a significant decrease in both TG Non-Ulcerated and TG Ulcerated when compared to TG muscles (Figure 22 E).

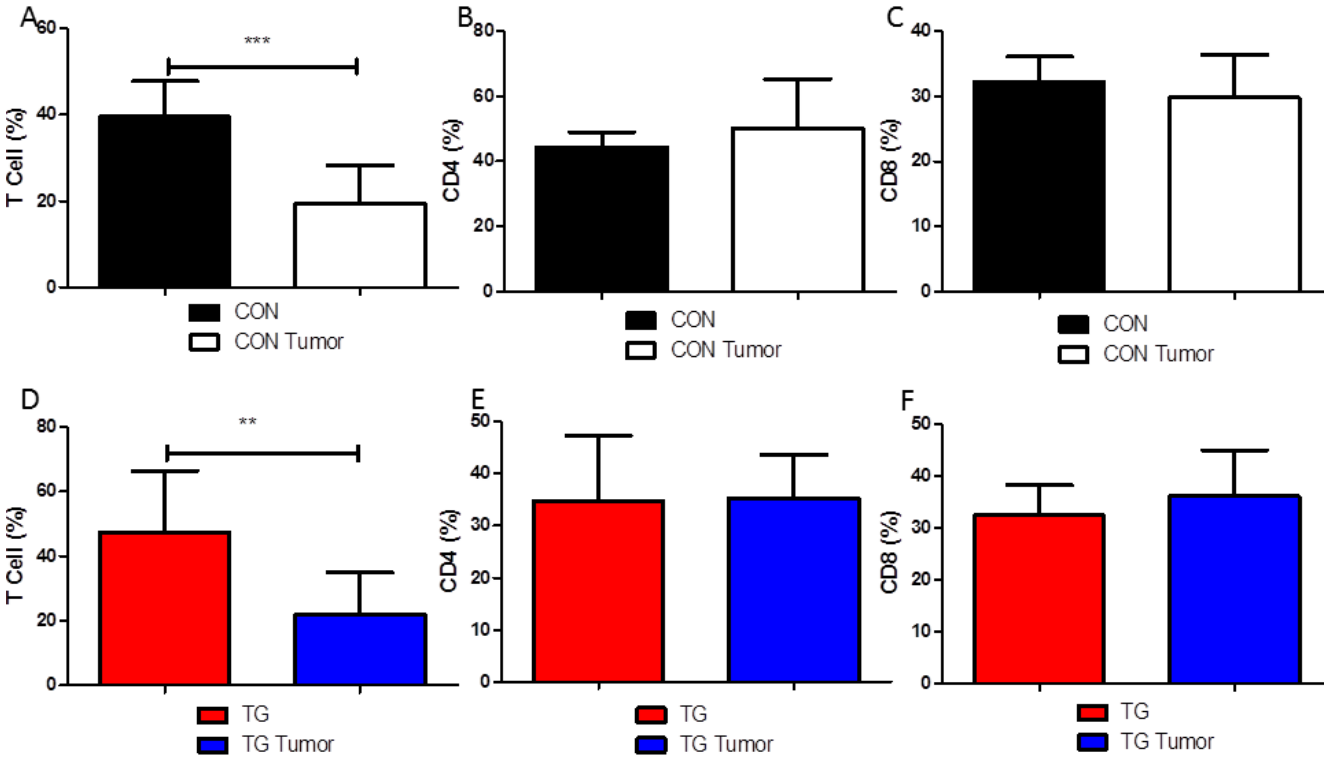

Figure 19 Spleen Cell Dissociation CON and TG: A. CON Tumor spleens showed a significant reduction in T cell % when compared to CON spleens. B., C. No statistical differences were seen between CD4% or CD8 % between groups. D. TG Tumor spleens showed a significant reduction in T cell % when compared to TG spleens. E., F. No statistical differences were seen between CD4% or CD8 % between groups CON (n=8), CON Non (n=8), CON Ulc (n=2), TG (n=7), TG Non (n=8), TG Ulc (n=4) *=P<0.05, **=P<0.005, ***=P<0.0001

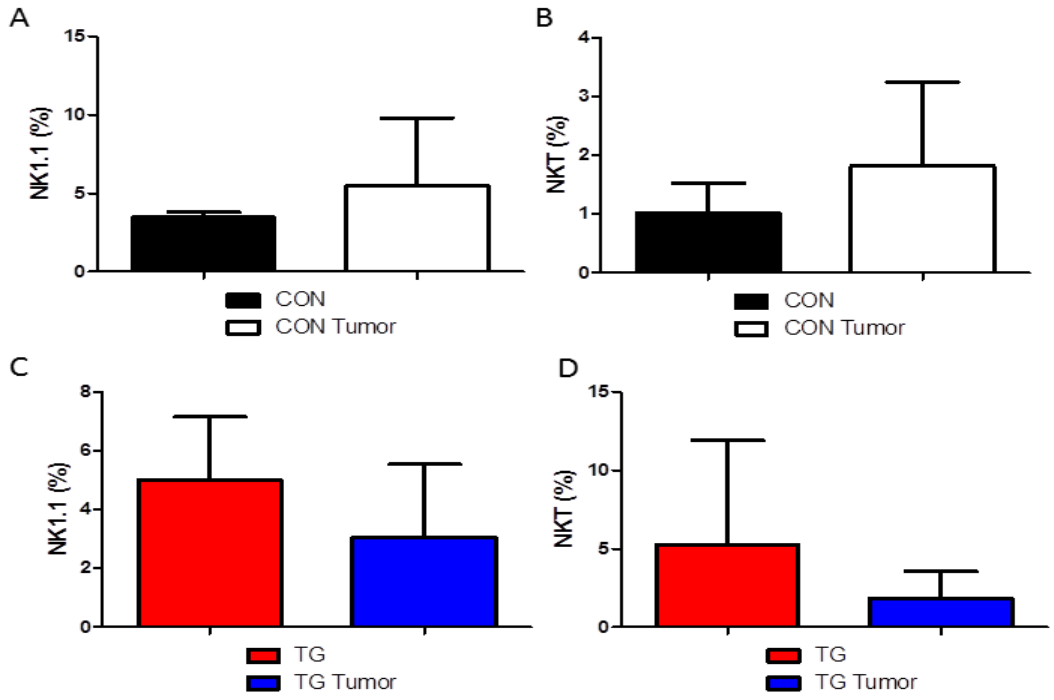

Figure 20 Spleen Dissociation CON and TG: No statistical differences were seen between groups in NK or NKT cells following spleen dissociation. CON (n=8), CON Non (n=8), CON Ulc (n=2), TG (n=7), TG Non (n=8), TG Ulc (n=4) *=P<0.05, **=P<0.005, ***=P<0.0001

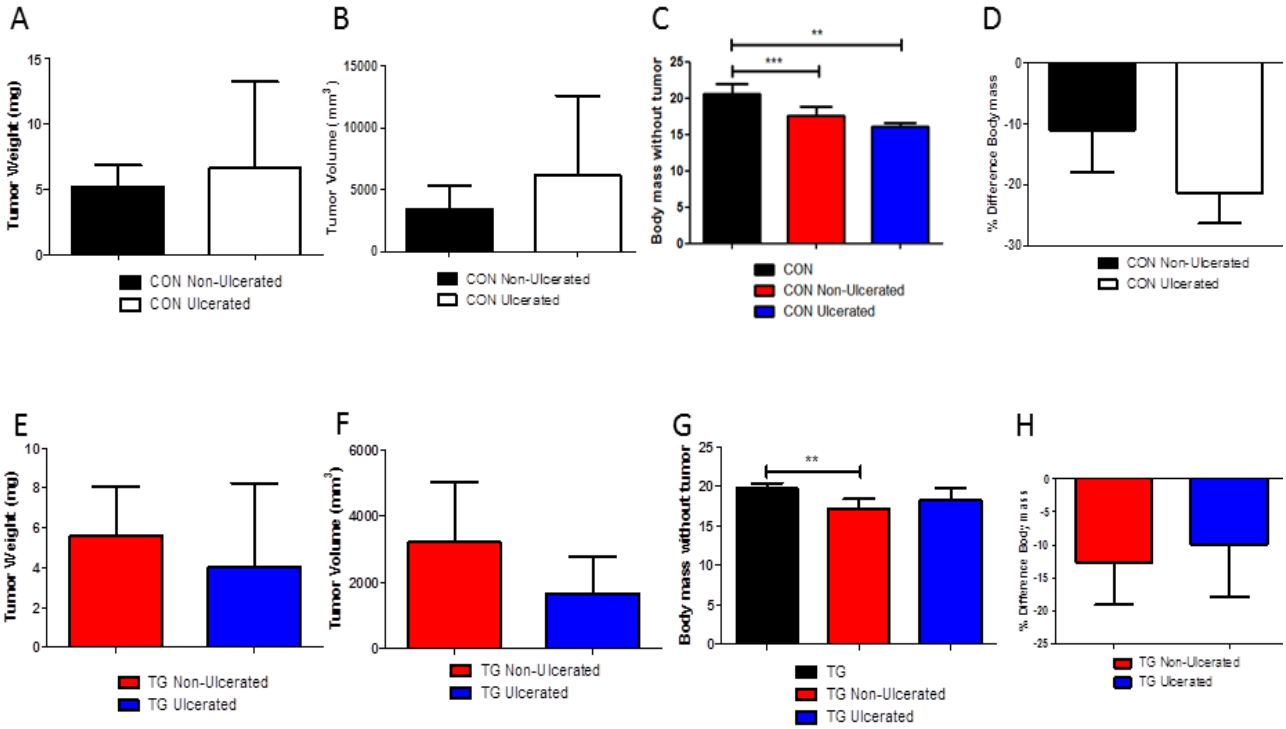

Figure 21 Tumor BW/Volume and Mouse Body mass: A., B., E., F., No statistical differences were seen between tumor weight or tumor volume in either CON or TG groups. C. Body mass with tumor removed showed a significant decrease in both CON Non-Ulcerated and CON Ulcerated compared to CON. G. TG Non-Ulcerated body mass without tumor showed a significant decrease when compared to TG mice. D., H. No statistical differences were seen between groups with regards to % difference in body mass. CON (n=8), CON Non (n=8), CON Ulc (n=2), TG (n=7), TG Non (n=8), TG Ulc (n=4) *=P<0.05, **=P<0.005, ***=P<0.0001

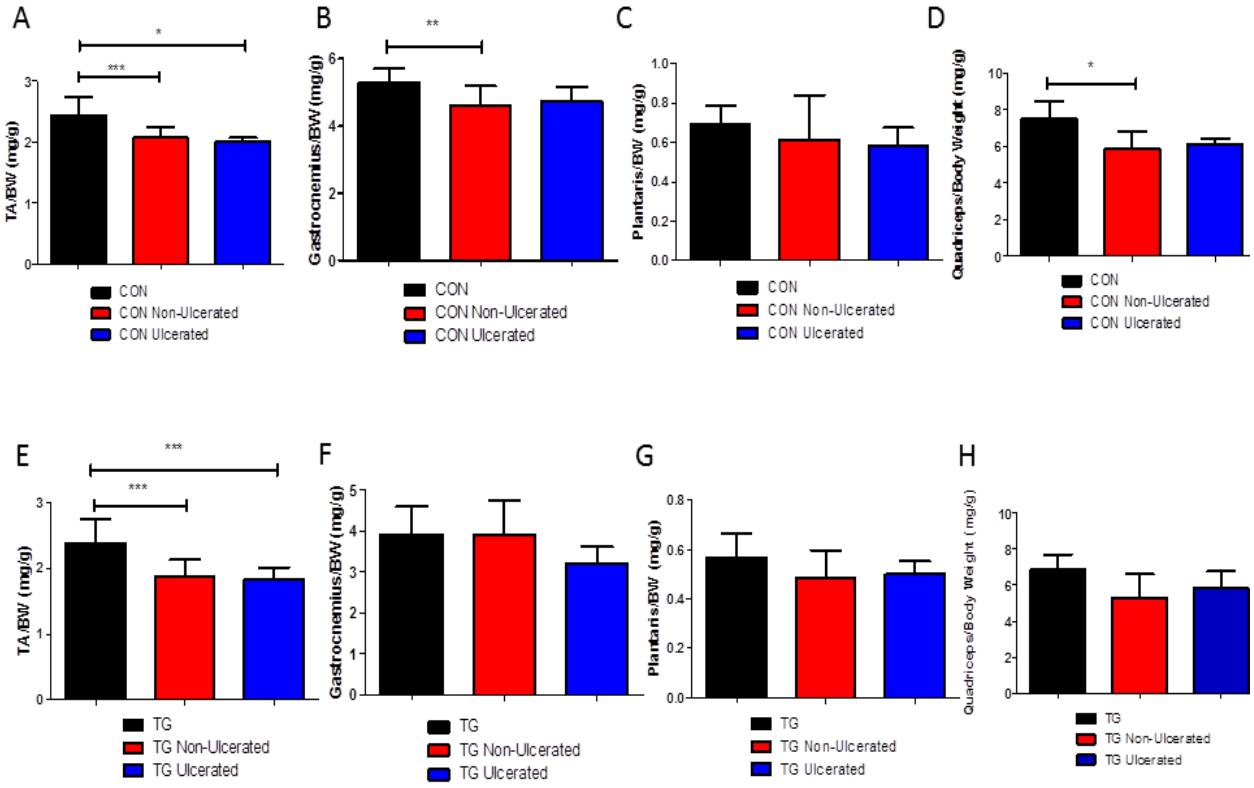

Figure 22 Muscle Weights/BW in CON and TG mice: A. TA/BW showed significant decreases in CON Non-Ulcerated and CON Ulcerated muscles compared to CON muscles. B. Gastroc/BW showed a significant decrease in CON Non-Ulcerated compared to CON muscles. C. No statistical differences were seen between Plantaris/BW. D. Quadriceps/BW showed a significant decrease in the CON Non-Ulcerated compared to CON muscles. E. TA/BW showed significant decreases in TG Non-Ulcerated and TG Ulcerated muscles compared to TG muscles. F., G., H. No statistical differences were seen between groups. CON (n=8), CON Non (n=8), CON Ulc (n=2), TG (n=7), TG Non (n=8), TG Ulc (n=4) *=P<0.05, **=P<0.005, ***=P<0.0001

Chapter 5

General Discussion

Injection of the EO771 mammary tumor cell line into C57BL/6 mice has been show to induce significant muscle wasting and muscle fatigue. This is verified by significant decreases in muscle weights as well as body weight, along with the increased fatigue shown at the 4-week post injection time point (Figure 2,4,7 and 8). Coinciding with the increased fatigue we showed a decreased mtDNA content (fold difference) in both 4-week time points suggesting these muscles are fatiguing more than the CON and 2WK due to less functional mitochondria. Indeed, our lab has shown the opposite of this where there is an increased mtDNA content via increases in secretion of IL-15 (23,39). In this model we also show a significant shift in the force frequency relationship in the EDL muscles of both 4WK Non-Ulcerated and Ulcerated groups(Figure 3 B) along with lower tetanus forces in both 4 week groups for both EDL and SOL. This shows that these muscles are not only fatiguing more, but they are producing greater forces at lower stimulation frequencies indicating overall muscle dysfunction and a more fatigable phenotype. Along with this we show significant increases in mRNA content for various biomarkers of atrophy (Murf1 and Atrogin1), inflammatory markers for cachexia (IL-6 and TNFα) and significant decreases in IL-15 and IL-15 rα which have proposed mechanisms behind mitochondrial biogenesis (40,41). We also show a significant shift in muscle fiber area in the EDL muscle after laminin staining in both the 4 week groups, supporting our claim that the muscles weight less and have a smaller CSA yielding less force and fatiguing at a more rapid rate than CON of 2WK mice. Our flow cytometry data from our spleen cell isolation did not show

significant differences; however when comparing just the CON and 2WK groups we saw a significant decrease in T cell % (Figure 10). The reasoning behind this notion is that the immune response generated by the cancer can be transient in the perspective of this study. Indeed, with this timeframe (4 weeks) the tumor has had time to bypass the immune system and shed potential targeting antigens (31,32). This could lend some insight as to why our deviations at the 4 week time points are so variable. These data show that the EO771 cell line induces cancer cachexia and muscle dysfunction (fatigue), and furthermore is an ideal model to test our proposed therapy of IL-15 skeletal muscle overexpression (Figure 5).

Previous work shows the ability of IL-15 to promote a pro-oxidative/fatigue resistant phenotype along with increasing overall mitochondrial density (38,40,41,53). It is by this mechanism that we propose our therapy will prevent the muscular fatigue in our model. With regards to muscle weights and CSA we saw similarities in the TG groups showing significant decreases in weight and CSA, coinciding with the preliminary study. The littermate controls showed a similarities in the CON Non-Ulcerated groups, however due to a small sample size (n=2) the CON Ulcerated group did not recapitulate the trend seen in our preliminary work (Figure 10). Looking at the functionality of the EDL muscle, TG CT and ½ RT showed significant decreases in both TG Non-Ulcerated and Ulcerated groups signifying alterations in Ca+ handling due to the systemic effects of the cancer (Figure 11). Again we did not see the same results represented in our CON groups, we believe this to be due to a small sample size. EDL muscles from both the CON and TG groups showed a significant decrease in muscle mass in the Non-Ulcerated and Ulcerated groups for absolute force frequency (Figure

12). This coincides with our previous study showing the EDL muscle producing less overall force in tumor bearing mice. Looking at the relative force frequency curve however, we show no shift in the CON group indicating the muscles are not producing greater force at lower frequencies which would indicate dysfunction. This is dissimilar to our preliminary study where, indeed we showed a significant shift in the force frequency curve. Possible explanations could be attributed to the small sample size, along with the fact these mice may have not been as severe as our previous study with regards to tumor burden. SOL muscles for both CON and TG showed a significant reduction in absolute force frequency similar to EDL muscles, however this was ablated when looking at relative force frequency. These data highlight the ability of a more oxidative muscle, even in the absence of IL-15 overexpression (i.e. littermate control) to preserve overall function in the presence of cancer cachexia. Of note, the SOL maximal tetanus contraction did show a significant decrease in the CON vs CON ulcerated group.

The major focus on this study was the attenuation of muscle fatigue in the presence of cancer cachexia. Using our fatigue protocol, we saw a significant shift down and to the left in force produced throughout our fatigue curve (% force loss) for both the CON Non-Ulcerated and CON Ulcerated mice vs CON (Figure 14). This shift was significant for contractions between 20-70 seconds showing a much more rapid and prolonged fatigue. In comparison, the TG fatigue curve showed a much smaller shift in Non-Ulcerated and Ulcerated mice, however still significant (Figure1 14). Of note this fatigue curve started later in the protocol (40 seconds) highlighting the attenuation of fatigue. It is important to note that these effects happened regardless of muscle mass loss, considering TG EDL muscles showed similar weight loss to our

preliminary study. Another method of analysis was looking at the overall area under the fatigue curve. We classify this as the total amount of force in mN throughout the 6 minute fatigue protocol. We see there was a significant reduction in area under the fatigue comparing the CON and CON Non-Ulcerated mice. This reinforces the idea that there is an increased fatigue in these mice (Figure 15). Again if we had more mice in the CON Ulcerated group we feel that we would have reached significance considering our preliminary study. Looking at the TG area under the fatigue curve we show no differences between groups, further exemplifying the attenuation of fatigue in these mice (Figure 15). These data suggest IL-15 has the ability to promote a fatigue resistant phenotype, attenuating overall fatigue experienced in cancer cachexia settings. When looking at the more oxidative muscle (SOL) we saw no significant differences in relative fatigue between either CON for TG groups, again showing preservation of function in a more mitochondrial dense muscle (Figure 16).

When we imaged these mice we saw a slight trend towards overall reduction of size in tumors of the TG groups, however it was not significant. IL-15 has been shown to promote overall immune function and cell cytotoxicity when treating cancer patients in clinical trials (54-56). However, previous work with this cell line has shown that the immunosuppressive nature of EO771 tumors can make it a challenging model to test immune based therapies (57). We showed a trend with reduction of tumor burden in the TG injected mice looking at tumor volume and IVIS bioluminescence, however there was no significance (Figure 17). Furthermore, we showed no statistical differences between the CON Tumor and TG Tumor following dissociation looking at different immune cells (CD4 Helper T, CD8 Cytotoxic T, NK1.1, NKT) (Figure 18). With the

spleen cell dissociation, we did show a significant reduction in T cells in the CON Tumor and TG Tumor when compared to their respective controls, however no other stains showed any significant differences (Figure 19 and 20). We attribute this to the immunosuppressive nature of this tumor type (57) as well as the tumors ability at this point to bypass any immune response. Further studies should be done looking at sooner time points (2WK) which would give us a better scope of the immune response with IL-15 treatment. Looking at overall tumor burden (weight/volume) we did not show any statistical differences between Non-Ulcerated or Ulcerated groups for either CON or TG mice (Figure 21 A, B, E, F). This could be a sample size issue considering the CON Ulcerated group had n=2 and the TG Ulcerated had N=4. We did show that the body mass of CON mice with the tumor removed was significantly lower in the CON Non-Ulcerated and CON Ulcerated, along with a large difference in body mass in the CON Ulcerated groups, however not significant (Figure 21 C,D). We did show a significant reduction in the TG Non-Ulcerated mass with tumor removed when compared to TG uninjected and we felt significance would be reached in the TG Ulcerated group if we increased the sample size (Figure 21). Tibialis Anterior muscle dissection is the most accurate and precise dissection next to EDL and SOL muscles. In the TA we showed significant reduction in CON Non-Ulcerated and CON Ulcerated weights compared to CON as well as significant reduction in TG Non-Ulcerated and TG Ulcerated compared to TG (Figure 22). These data combine with our previous measurements show an overall decrease in muscle weight with the presence of cancer.

While we did not show differences in immune function, we were able to attenuate muscle fatigue in the presence of cancer due to IL-15 skeletal muscle overexpression.

These effects can be very translational due to IL-15 testing already taking place in clinical trials for improving immune function in cancer patients (7,54-56). With this in mind IL-15 can be proposed as an effective dual immune/fatigue therapy by primarily targeting improvements in immune function all while attenuation skeletal muscle fatigue seen in cancer cachexia patients. This becomes crucial when treatment of the cancer takes place. With chemotherapy potentially exacerbating cachexia, the ability to attenuate fatigue and improve immune response will likely lead to a faster recovery and decreased morbidity and mortality.

The next step for this project would be the addition of mice to both 4WK Ulcerated groups. This would give us an overall even number in each group, potentially allowing our littermate control data to recapitulate our preliminary research. Additionally we plan to dissociate more tumors in the 4WK groups, as well as establishing a 1 and 2 week time point. We feel the addition of these groups will potentially lead to our further understanding of the effects IL-15 has in the immune response in our particular model.

Our next proposed step would be the administration of IL-15 via osmotic mini pump. After a preliminary trial using an IL-15 administered group (n=2) and a sham groups given sterile PBS (n=2) we were able to perform a sterile surgery and have mice survive to the 4 week time point. Moving forward we plan to repeat the protocol both addressing different dose dependent alterations in muscle function and immune cell populations, but also identifying any toxic or inflammatory responses associated with this method of administration. Indeed, previous work in cancer patients who were administered human IL-15 showed positive responses in CD8 T cell and NK cell activity. Higher doses however, were also associated with increased toxicity and a larger

inflammatory response (55). This will allow us to identify a dose that will produce the best response in attenuating muscle fatigue. Following this we can scale up dosing to address muscle fatigue in a clinical setting of cancer cachexia

Chapter 5

Methodology

6.1

Mice

C57BL6WT mice were purchased from The Jackson Laboratory (n=23) and randomly assigned to a control group (Control; n=8), mice that were euthanized following 2 weeks of tumor growth (2WK, n=5), and mice that were euthanized following 4 weeks of tumor growth (4WK, n=10). The 4WK group was subsequently divided into mice that developed an ulcerated tumor (4WK-UT; n=6) and mice that developed a non-ulcerated tumor (4WK-NUT; n=4). IL-15 TG muscle overexpressor mice were purchased from Jackson Laboratory and bred yielding IL-15 TG overexpressor pups and littermate controls, which were used for the subsequent experiment. Mice were split into six groups; a control uninjected group (CON=8), a control Ulcerated group (CON Non-Ulcerated=8), a Control Ulcerated group (CON Ulcerated= 2), a transgenic group (TG=7), a transgenic Non-Ulcerated group (TG Non-Ulcerated=7) and transgenic Ulcerated group (TG Ulcerated=4) Mice were housed in the animal vivarium at West Virginia University at 22°C under a 12:12-h light-dark cycle and received food and water ab libitum. All animal experiments were approved by the Institutional Animal Care and Use Committee at West Virginia University.

6.2

E0771 Murine Breast Cancer Cells

The E0771 cell line used in these studies was kindly provided by Linda Metheney-Barlow (Wake Forest) E0771 cells were cultured using aseptic technique and maintained under standard mammalian culture conditions (37ºC, 99% humidity, 5% CO2). Cells were maintained in high glucose DMEM supplemented with 10% FBS to maintain active proliferation. Cells were passed via trypsinization using 0.25% trypsin/EDTA in Hanks buffered saline solution (Gibco). Cells were grown until ~90% confluent at which time they were prepped for injection. Cells were trypsinized and resuspended in sterile PBS. A cell count was performed yielding 1 million cells per 100µL injection into the 4th nipple (mammary fat pad) of female C57BL6WT mice and IL-15 TG mice.

6.3

Muscle Physiology on EDL and SOL Muscle in C57BL6WT mice and IL-15 TG overexpression mice.

Female mice were deeply anesthetized by breathing 4% isoflurane delivered through a nose cone at a flow rate of 1 l/min. Muscles were removed with both proximal and distal tendons intact, and nylon sutures were attached to the tendons. Muscles were transferred to an oxygenated tissue bath that contained Ringer solution (100 mM NaCl, 4.7 mM KCl, 3.4 mM CaCl2, 1.2 mM KH2PO4, 1.2 mM MgSO4, 25 mM HEPES, and 5.5 mM D-glucose) maintained at 22°C. Ex vivo muscle stimulation was performed using a commercially available muscle physiology system (Aurora Scientific, Ontario, CA). Muscle length was adjusted to obtain the maximal twitch response (i.e., Lo). Three

twitch contractions were performed all separated by 2 min. Parameters analyzed from isometric contractions included peak isometric twitch force (Pt), time to peak twitch tension (TPT), half-relaxation time of twitch contraction (½ RT), and peak isometric tetanic force (Po). Isometric tetanic contractions were stimulated in muscles at a stimulation frequency of 120 Hz for EDL muscles and 80 Hz for soleus muscles, a stimulation current of 20 V, and lasting 500 ms. Following isometric contractions, the muscles remained in oxygenated Ringer's for 5 minutes prior to the repeated-stimulation fatigue protocol. Muscle fatigue was analyzed using a repeated stimulation protocol lasting 6 min and consisting of repeated 40-Hz tetanic trains that occurred once every second and lasted 330 ms.

6.4

Muscle Morphology

Due to our previous reports showing a decrease in fiber area with progression of cancer cachexia EDL and SOL muscles will be flash frozen in isopentane cooled to the temperature of liquid nitrogen and stored at –80°C. Serial frozen sections (10 μm thick) of EDL and SOL muscles were obtained using a cryostat at −21°C and placed onto glass slides (Superfrost/Plus, Fisher Scientific). Sections were stained with Alexa Flour® 488-conjugate AffiniPure Goat Anti-Rabbit IgG (Jackson ImmunoResearch Labratories, INC) and ANTI-LAMININ Affinity Isolated Antigen Specific Antibody(SIGMA-ALDRICH®) and then mounted with 4',6-diamidino-2-phenylindole (DAPI) mounting medium (Vector Laboratories, Burlingham, CA). Similar Analysis will

be performed using the Image Process & Analysis Workstation in the CORES Facility, utilizing the Muscle Fiber General Analysis protocol.

6.5

Mitochondrial DNA content

Total DNA (genomic and mitochondrial) will be extracted from tibialis anterior (TA) muscles from female mice using a DNeasy Blood and Tissue kit (Qiagen, Valencia, CA) and quantified using a Nano-Drop spectrophotometer (ThermoScientific, Waltham, MA). TaqMan primers for mitochondrial DNA-encoded cytochrome-c oxidase subunit II (COXII) and nuclear-encoded 18S ribosomal RNA will be used to perform real-time qPCR. The wells of a 96-well optical reaction plate were loaded with a 20-µl volume consisting of TaqMan 10X PCR Master Mix, a primer mix for either the mitochondrial-encoded gene or the nuclear-encoded gene, and DNA diluted to a concentration of 5 ng/µl. Each DNA sample was analyzed in pairs and amplified in an Applied Biosystems 7900HT Fast Real-Time PCR system. The cycle threshold (CT) values of the mitochondrial-encoded COXII gene and the nuclear-encoded 18S gene in muscles C57BL6 WT mice were used to quantify the fold change using the ΔΔCT calculation (58)

6.6

RNA Isolation and PCR

Total RNA will be isolated using Trizol reagent (Life Technologies, Grand Island, NY), as previously described (59). RNA quantity and quality will be assessed using a Nano-

Drop 2000 spectrophotometer (ThermoScientific, Waltham, MA); the 260/280 ratio for all samples used was between 1.8 and 2.1. Two micrograms of total RNA will be reverse transcribed to make cDNA using a high-capacity reverse transcription kit according to manufacturer's instructions (Life Technologies, Grand Island, NY). Amplification was performed in a reaction consisting of 8.5 µl nuclease-free H2O, 12.5 µl 2X Taq-Pro Red Complete 1.5 mM MgCl2 master mix (Denville Scientific, Metuchen, NJ), 1.0 µl forward primer, 1.0 µl reverse primer, and 2 µl of DNA template to make a 25 µl total reaction volume. Primers were constructed from published sequences. Primer pairs for IL-15, IL-15 rα, IL-6, TNFα, Grim19, Murf1 and Atrogin-1 were coamplified with primer pairs for 18S (Ambion, Austin, TX). The number of PCR cycles was determined in preliminary experiments to ensure analyses were done in the linear range of amplification. Following amplification, each reaction will be visualized following gel electrophoresis in 1% (wt/vol) agarose gels stained with ethidium bromide. PCR bands were quantified using the ImageJ software program (http://rsbweb.nih.gov/ij/). Signals for the gene of interest were normalized to the bands for 18S that were amplified in the same reaction.

6.7

Spleen Cell Isolation

Single cell suspensions from the spleen and of each mouse were extracted and a single cell suspension of 1 million cells will be generated following cell isolation, red blood cell lysing and washing steps (1.5% FBS RPMI). Staining will comprise of CD3 (generalized T cell marker), CD4 (Helper T cell marker), CD8 (Cytotoxic T cell) and Natural Killer cell

staining (NK). T cell count will be gated to a CD45 cell surface marker antibody. Flow data gives us a representative image of the percent of cells in solution.

6.8

Tumor Dissociation

Tumors will be dissected away from mice and homogenized using the MACS tissue dissociator. (MACS Miltenyi Biotec). Following dissociation cells will be strained and the red blood cells with be lysed. Following a period of wash steps similar to the spleen cell isolation, 1 million cells will be collected and stained for flow cytometry. Staining will comprise of CD3 (generalized T cell marker), CD4 (Helper T cell marker), CD8 (Cytotoxic T cell) and Natural Killer cell staining (NK). T cell count will be gated to a CD45 cell surface marker antibody. Flow data will give us a representative image of the percent of cells in solution.

6.9

IVIS Imagine and Tumor Burden

Imaging of each mouse will take place once a week in the Animal Facility. A luciferase injection will be administered so the EO771 cells illuminate during recording. Mice will be anesthetized by breathing 4% isoflurane delivered through a nose cone at a flow rate of 1 l/min. The subsequent images generated from this will be analyzed looking at tumor growth and total flux score.

6.10

VEVO Tumor Volume

Following IVIS Imaging, mice will be transferred to the VEVO Ultrasound room. Mice will be anesthetized by breathing 4% isoflurane delivered through a nose cone at a flow rate of 1 l/min. Tumor volume will be measured using ultrasound (Visual Sonics) and tumor volumes calculated from these data.

6.11

Data Collection

Statistical analysis was performed using GraphPad Prism 5 software. Data will be reported as mean ± SEM, using ANOVA statistical analysis between experimental groups and student t-test where applicable.

6.12

Animal Care

Mice were housed in the Animal Resources Department of West Virginia University School of Medicine in compliance with the NIH and the Institutional Animal Care and Use Committee guidelines. Animals are attended by a full-time veterinary and support staff. Unless noted otherwise, the animals are house in a pathogen-free environment, receive food and water ad libitum, and receive standard care daily.

Chapter 7

References

1. Tisdale, M. J. (2002) Cachexia in cancer patients. Nature Reviews Cancer 2, 862-871

2. Zhou, X., Wang, J. L., Lu, J., Song, Y., Kwak, K. S., Jiao, Q., Rosenfeld, R., Chen, Q., Boone, T., and Simonet, W. S. (2010) Reversal of cancer cachexia and muscle wasting by ActRIIB antagonism leads to prolonged survival. Cell 142, 531-543

3. Laviano, A., Inui, A., Marks, D. L., Meguid, M. M., Pichard, C., Fanelli, F. R., and Seelaender, M. (2008) Neural control of the anorexia-cachexia syndrome. American Journal of Physiology-Endocrinology and Metabolism 295, E1000-E1008

4. Grossberg, A. J., Scarlett, J. M., and Marks, D. L. (2010) Hypothalamic mechanisms in cachexia. Physiology & behavior 100, 478-489

5. Acharyya, S., Ladner, K. J., Nelsen, L. L., Damrauer, J., Reiser, P. J., Swoap, S., and Guttridge, D. C. (2004) Cancer cachexia is regulated by selective targeting of skeletal muscle gene products. The Journal of clinical investigation 114, 370-378

6. Lynch, G. S. (2001) Therapies for improving muscle function in neuromuscular disorders. Exercise and sport sciences reviews 29, 141-148

7. Pagliari, D., Frosali, S., Landolfi, R., and Cianci, R. (2013) The role of IL-15 in human cancer: friend or foe? International Trends in Immunity 1, 35-42

8. Gullett, N., Rossi, P., Kucuk, O., and Johnstone, P. A. (2009) Cancer-induced cachexia: a guide for the oncologist. Journal of the Society for Integrative Oncology 7

9. Tisdale, M. J. (2009) Mechanisms of cancer cachexia. Physiological reviews 89, 381-410

10. Fearon, K. C., Glass, D. J., and Guttridge, D. C. (2012) Cancer cachexia: mediators, signaling, and metabolic pathways. Cell metabolism 16, 153-166

11. Lundholm, K., Korner, U., Gunnebo, L., Sixt-Ammilon, P., Fouladiun, M., Daneryd, P., and Bosaeus, I. (2007) Insulin treatment in cancer cachexia: effects on survival, metabolism, and physical functioning. Clinical cancer research : an official journal of the American Association for Cancer Research 13, 2699-2706

12. Del Fabbro, E., Hui, D., Dalal, S., Dev, R., Nooruddin, Z. I., and Bruera, E. (2011) Clinical outcomes and contributors to weight loss in a cancer cachexia clinic. Journal of palliative medicine 14, 1004-1008

13. Fearon, K. C. (2008) Cancer cachexia: developing multimodal therapy for a multidimensional problem. European journal of cancer 44, 1124-1132

14. Busquets, S., Carbo, N., Almendro, V., Figueras, M., Lopez-Soriano, F. J., and Argiles, J. M. (2001) Hyperlipemia: a role in regulating UCP3 gene expression in skeletal muscle during cancer cachexia? FEBS letters 505, 255-258

15. Toledo, M., Penna, F., Oliva, F., Luque, M., Betancourt, A., Marmonti, E., López-Soriano, F. J., Argilés, J. M., and Busquets, S. (2015) A multifactorial anti-cachectic approach for cancer cachexia in a rat model undergoing chemotherapy. Journal of cachexia, sarcopenia and muscle

16. Evans, W. J., Morley, J. E., Argiles, J., Bales, C., Baracos, V., Guttridge, D., Jatoi, A., Kalantar-Zadeh, K., Lochs, H., Mantovani, G., Marks, D., Mitch, W. E., Muscaritoli, M., Najand, A., Ponikowski, P., Rossi Fanelli, F., Schambelan, M., Schols, A., Schuster, M., Thomas, D., Wolfe, R., and Anker, S. D. (2008) Cachexia: a new definition. Clinical nutrition 27, 793-799

17. Kollias, G., Douni, E., Kassiotis, G., and Kontoyiannis, D. (1999) On the role of tumor necrosis factor and receptors in models of multiorgan failure, rheumatoid arthritis, multiple sclerosis and inflammatory bowel disease. Immunological reviews 169, 175-194

18. Balkwill, F., and Mantovani, A. (2001) Inflammation and cancer: back to Virchow? Lancet 357, 539-545

19. Cahlin, C., Korner, A., Axelsson, H., Wang, W., Lundholm, K., and Svanberg, E. (2000) Experimental cancer cachexia: the role of host-derived cytokines interleukin (IL)-6, IL-12, interferon-gamma, and tumor necrosis factor alpha evaluated in gene knockout, tumor-bearing mice on C57 Bl background and eicosanoid-dependent cachexia. Cancer research 60, 5488-5493

20. Langstein, H. N., and Norton, J. A. (1991) Mechanisms of cancer cachexia. Hematology/oncology clinics of North America 5, 103-123

21. Guo, Y., Xu, F., Lu, T., Duan, Z., and Zhang, Z. (2012) Interleukin-6 signaling pathway in targeted therapy for cancer. Cancer treatment reviews 38, 904-910

22. Bodine, S. C., and Baehr, L. M. (2014) Skeletal muscle atrophy and the E3 ubiquitin ligases MuRF1 and MAFbx/atrogin-1. American Journal of Physiology-Endocrinology and Metabolism 307, E469-E484

23. O'Connell, G. C., and Pistilli, E. E. (2015) Interleukin-15 directly stimulates pro-oxidative gene expression in skeletal muscle in-vitro via a mechanism that requires interleukin-15 receptor alpha. Biochemical and biophysical research communications 458, 614-619

24. Julienne, C. M., Dumas, J. F., Goupille, C., Pinault, M., Berri, C., Collin, A., Tesseraud, S., Couet, C., and Servais, S. (2012) Cancer cachexia is associated with a decrease in skeletal muscle mitochondrial oxidative capacities without alteration of ATP production efficiency. Journal of cachexia, sarcopenia and muscle 3, 265-275

25. Coats, V., Ribeiro, F., Tremblay, L., Fortin, B., Maltais, F., and Saey, D. (2015) Mid-thigh cross-sectional area and lower limb muscle function in patients with lung cancer. European Respiratory Journal 46, PA1552

26. Timonen, T., and Herberman, R. (1981) Characteristics of human large granular lymphocytes and relationship to natural killer and K cells. The Journal of experimental medicine 153, 569-582

27. Albertsson, P. A., Basse, P. H., Hokland, M., Goldfarb, R. H., Nagelkerke, J. F., Nannmark, U., and Kuppen, P. J. (2003) NK cells and the tumour microenvironment: implications for NK-cell function and anti-tumour activity. Trends in immunology 24, 603-609

28. Pardoll, D. M., and Topalian, S. L. (1998) The role of CD4+ T cell responses in antitumor immunity. Current opinion in immunology 10, 588-594

29. Riddell, S. R., and Greenberg, P. D. (1995) Principles for adoptive T cell therapy of human viral diseases. Annual review of immunology 13, 545-586

30. Trinchieri, G. (2012) Cancer and inflammation: an old intuition with rapidly evolving new concepts. Annual review of immunology 30, 677-706

31. Finn, O. J. (2012) Immuno-oncology: understanding the function and dysfunction of the immune system in cancer. Annals of oncology : official journal of the European Society for Medical Oncology / ESMO 23 Suppl 8, viii6-9

32. Noh, K. H., Kim, S.-H., Kim, J. H., Song, K.-H., Lee, Y.-H., Kang, T. H., Han, H. D., Sood, A. K., Ng, J., and Kim, K. (2014) API5 confers tumoral immune escape through FGF2-dependent cell survival pathway. Cancer research 74, 3556-3566

33. Bruera, E., Roca, E., Cedaro, L., Carraro, S., and Chacon, R. (1985) Action of oral methylprednisolone in terminal cancer patients: a prospective randomized double-blind study. Cancer treatment reports 69, 751-754

34. Esper, D. H., and Harb, W. A. (2005) The cancer cachexia syndrome: a review of metabolic and clinical manifestations. Nutrition in clinical practice : official publication of the American Society for Parenteral and Enteral Nutrition 20, 369-376

35. Moore, R., Owens, D., Stamp, G., Arnott, C., Burke, F., East, N., Holdsworth, H., Turner, L., Rollins, B., and Pasparakis, M. (1999) Tumour necrosis factor-a deficient mice are resistant to skin carcinogenesis. Nat Med 5, 828-831

36. Malik, S. T., Griffin, D. B., Fiers, W., and Balkwill, F. R. (1989) Paradoxical effects of tumour necrosis factor in experimental ovarian cancer. International journal of cancer. Journal international du cancer 44, 918-925

37. Tricot, G. (2000) New insights into role of microenvironment in multiple myeloma. Lancet 355, 248-250

38. Pistilli, E. E., Bogdanovich, S., Garton, F., Yang, N., Gulbin, J. P., Conner, J. D., Anderson, B. G., Quinn, L. S., North, K., Ahima, R. S., and Khurana, T. S. (2011) Loss of IL-15 receptor alpha alters the endurance, fatigability, and metabolic characteristics of mouse fast skeletal muscles. The Journal of clinical investigation 121, 3120-3132

39. Pistilli, E. E., Guo, G., and Stauber, W. T. (2013) IL-15Rα deficiency leads to mitochondrial and myofiber differences in fast mouse muscles. Cytokine 61, 41-45

40. Quinn, L. S., Haugk, K., and Grabstein, K. (1995) Interleukin-15: a novel anabolic cytokine for skeletal muscle. Endocrinology 136, 3669-3672

41. Quinn, L. S., Anderson, B. G., Conner, J. D., and Wolden-Hanson, T. (2012) IL-15 overexpression promotes endurance, oxidative energy metabolism, and muscle PPARδ, SIRT1, PGC-1α, and PGC-1β expression in male mice. Endocrinology 154, 232-245

42. Kennedy, M. K., Glaccum, M., Brown, S. N., Butz, E. A., Viney, J. L., Embers, M., Matsuki, N., Charrier, K., Sedger, L., Willis, C. R., Brasel, K., Morrissey, P. J., Stocking, K., Schuh, J. C., Joyce, S., and Peschon, J. J. (2000) Reversible defects in natural killer and memory CD8 T cell lineages in interleukin 15-deficient mice. The Journal of experimental medicine 191, 771-780

43. Lodolce, J. P., Boone, D. L., Chai, S., Swain, R. E., Dassopoulos, T., Trettin, S., and Ma, A. (1998) IL-15 receptor maintains lymphoid homeostasis by supporting lymphocyte homing and proliferation. Immunity 9, 669-676

44. Ranson, T., Vosshenrich, C. A., Corcuff, E., Richard, O., Müller, W., and Di Santo, J. P. (2003) IL-15 is an essential mediator of peripheral NK-cell homeostasis. Blood 101, 4887-4893

45. Ice, R. J., McLaughlin, S. L., Livengood, R. H., Culp, M. V., Eddy, E. R., Ivanov, A. V., and Pugacheva, E. N. (2013) NEDD9 depletion destabilizes Aurora A kinase and heightens the efficacy of Aurora A inhibitors: implications for treatment of metastatic solid tumors. Cancer research 73, 3168-3180

46. Ciciliot, S., Rossi, A. C., Dyar, K. A., Blaauw, B., and Schiaffino, S. (2013) Muscle type and fiber type specificity in muscle wasting. The international journal of biochemistry & cell biology 45, 2191-2199

47. Murphy, K. T., Chee, A., Trieu, J., Naim, T., and Lynch, G. S. (2012) Importance of functional and metabolic impairments in the characterization of the C-26 murine model of cancer cachexia. Disease models & mechanisms 5, 533-545

48. Gorselink, M., Vaessen, S. F., van der Flier, L. G., Leenders, I., Kegler, D., Caldenhoven, E., van der Beek, E., and van Helvoort, A. (2006) Mass-dependent decline of skeletal muscle function in cancer cachexia. Muscle & nerve 33, 691-693

49. Roberts, B., Frye, G., Ahn, B., Ferreira, L., and Judge, A. (2013) Cancer cachexia decreases specific force and accelerates fatigue in limb muscle. Biochemical and biophysical research communications 435, 488-492

50. Pfaffl, M. W. (2001) A new mathematical model for relative quantification in real-time RT-PCR. Nucleic acids research 29, e45

51. Acharyya, S., Butchbach, M. E., Sahenk, Z., Wang, H., Saji, M., Carathers, M., Ringel, M. D., Skipworth, R. J., Fearon, K. C., Hollingsworth, M. A., Muscarella, P., Burghes, A. H., Rafael-Fortney, J. A., and Guttridge, D. C. (2005) Dystrophin glycoprotein complex dysfunction: a regulatory link between muscular dystrophy and cancer cachexia. Cancer cell 8, 421-432

52. Quinn, L. S., Anderson, B. G., Strait-Bodey, L., Stroud, A. M., and Argilés, J. M. (2009) Oversecretion of interleukin-15 from skeletal muscle reduces adiposity. American Journal of Physiology-Endocrinology and Metabolism 296, E191-E202

53. Quinn, L., Anderson, B., Conner, J., Pistilli, E., and Wolden-Hanson, T. (2011) Overexpression of interleukin-15 in mice promotes resistance to diet-induced obesity, increased insulin sensitivity, and markers of oxidative skeletal muscle metabolism. Int J Infereron Cytokine Mediator Res 3, 29-42

54. Waldmann, T. A., Conlon, K. C., Stewart, D. M., Worthy, T. A., Janik, J. E., Fleisher, T. A., Albert, P. S., Figg, W. D., Spencer, S. D., and Raffeld, M. (2013) Phase 1 trial of IL-15 trans presentation blockade using humanized Mik-Beta-1 mAb in patients with T-cell large granular lymphocytic leukemia. Blood 121, 476-484

55. Conlon, K. C., Lugli, E., Rosenberg, S. A., Morris, J. C., Fleisher, T., Welles, H., Dubois, S., Perera, L., Goldman, C., and Bryant, B. (2014) Results from the first-in-human phase I trials of recombinant human Interleukin 15 (rhIL-15) administered as a daily 30 minute intravenous infusion (IVB) for 12 consecutive days or as continuous intravenous infusion (CIV) for 240 hours in patients with refractory metastatic cancers. Cancer research 74, 2575-2575

56. Hong, E., Usiskin, I. M., Bergamaschi, C., Hanlon, D. J., Edelson, R. L., Justesen, S., Pavlakis, G. N., Flavell, R. A., and Fahmy, T. M. (2015) Configuration-dependent presentation of multivalent IL-15: IL-15Rα enhances the antigen-specific T cell response and anti-tumor immunity. Journal of Biological Chemistry, jbc. M115. 695304

57. EWENS, A., MIHICH, E., and EHRKE, M. J. (2005) Distant metastasis from subcutaneously grown E0771 medullary breast adenocarcinoma. Anticancer research 25, 3905-3915

58. Arocho, A., Chen, B., Ladanyi, M., and Pan, Q. (2006) Validation of the 2-ΔΔCt calculation as an alternate method of data analysis for quantitative PCR of BCR-ABL P210 transcripts. Diagnostic Molecular Pathology 15, 56-61

59. Pistilli, E. E., Jackson, J. R., and Alway, S. E. (2006) Death receptor-associated pro-apoptotic signaling in aged skeletal muscle. Apoptosis : an international journal on programmed cell death 11, 2115-2126

Chapter 8

Supplemental Data

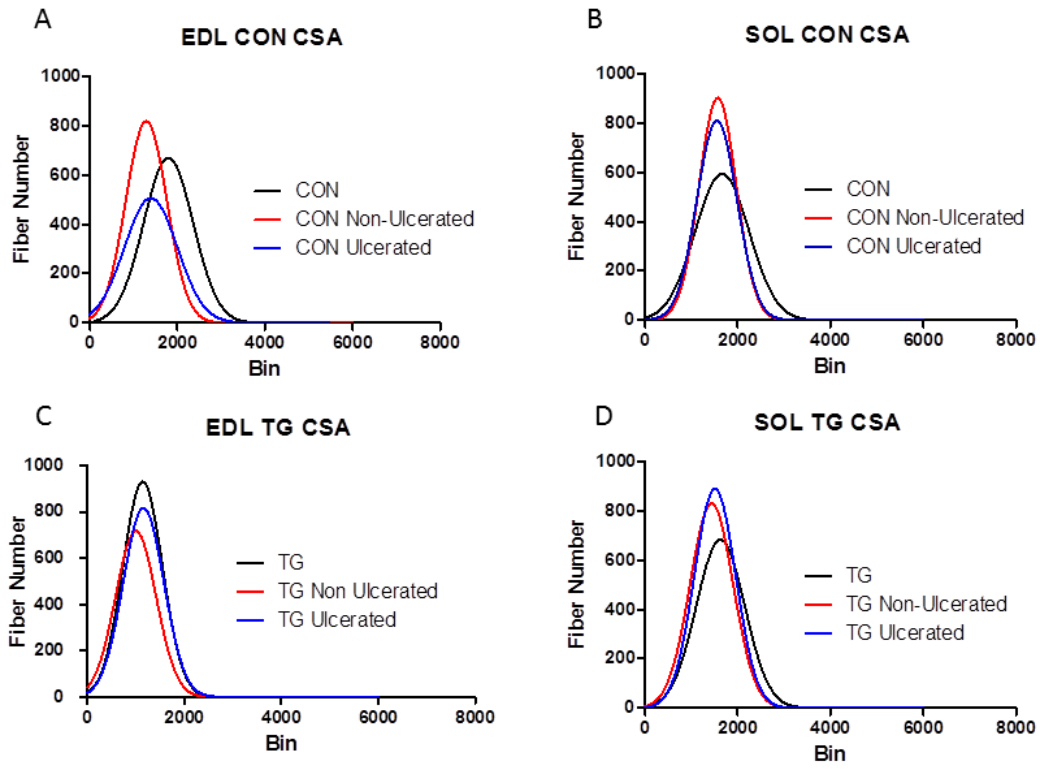

Supplemental 1 EDL and SOL Fiber Distribution: A. EDL CON Fiber Area showed a shift in both the CON Non-Ulcerated and CON Ulcerated groups compared to CON muscles. B. No differences were seen in SOL CON Fiber Area. C. No differences were seen in the EDL TG Fiber Area. D. No differences were seen in the SOL TG Fiber Area

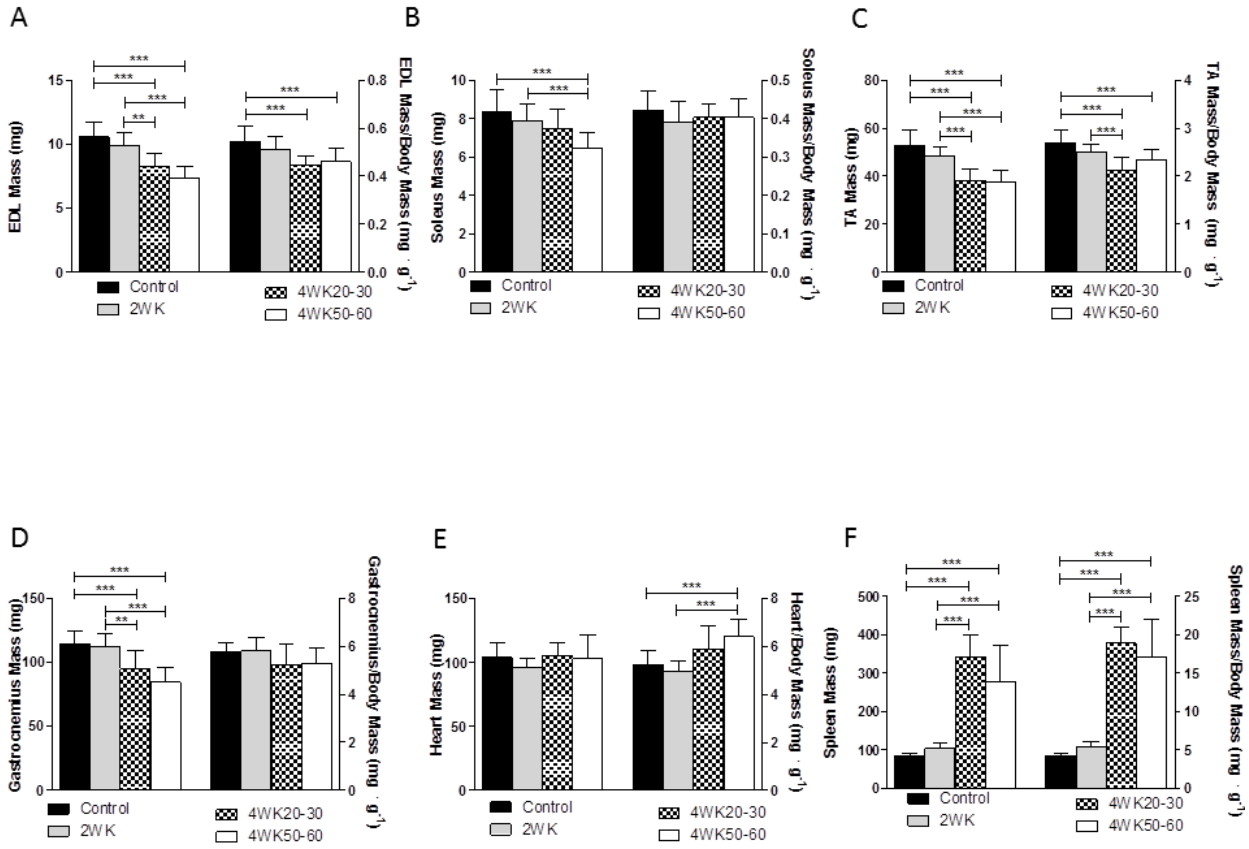

Supplemental 2: A. EDL absolute mass showing significant decreases in both 4 week groups compared to CON and 2WK, ELD mass normalized to body mass without the tumor showed significant decreases in both 4 week groups compared to CON mice. B. Absolute Soleus mass showed significant decreases in the 4 week Ulcerated groups compared to CON. C. TA absolute mass showed significant decreases in both 4 week groups compared to CON and 2 week, TA mass normalized to body mass without the tumor showed significant decreases in both 4 week groups compared to CON and 2 week. D. Gastrocnemius absolute mass showed significant decreases in both 4 week groups compared to CON and 2 week. E. Hear mass normalized to body mass without the tumor showed a significant increase in 4 week ulcerated mass compared to CON and 2 week. F. Both Absolute and normalized to body mass without the tumor weights of the spellen showed significant increases in the 4 week groups compared to the CON and 2 week groups